国科大杭州高等研究院
Hangzhou Institute For Advanced Study,UCAS

Compact star matter after GW170817

马永亮
国科大杭州高等研究院


國科大杭州高等研究院
Hangzhou Institute for Advanced Study, UCAS
美丽
西湖

国科大杭高院数理学院一瞥

中国科学院
CHINESE ACADEMY OF SCIENCES

浙江省人民政府
The People's Government of Zhejiang Province

中国科学院大学
University of Chinese Academy of Sciences

杭州
HANGZHOU

理事会

直属
二级学院

正局级
事业单位

国科大杭州高等研究院
Hangzhou Institute For Advanced Study,UCAS

国科大杭高院数理学院一瞥

国科大

采用深度科教融合建设模式

相互依托、资源共享、人员互聘

中科院研究所

杭高院二级学院和承办研究所的关系

1.杭高院每个二级学院由中科院1-2个研究所重点支持共建。

2.杭高院和研究所是相互依托、资源共享，合作共赢、错位发展的建设共同体。

3.杭高院师资力量由杭高院全职及来自承办学院的中科院相关研究所的双聘教授组成。

杭高院二级学院

国科大杭高院数理学院一瞥

国科大杭州高等研究院
Hangzhou Institute For Advanced Study,UCAS

- 过渡校区与云栖小镇国际会展中心比邻而居，附近聚集有西湖大学、之江实验室、中国美术学院、浙江音乐学院等院校机构

- 永久校区将与现已开工建设中的铜鉴湖4A级景区无缝连接，融为一体，并紧邻地铁6号线双浦站，兼具山水风光和便捷交通

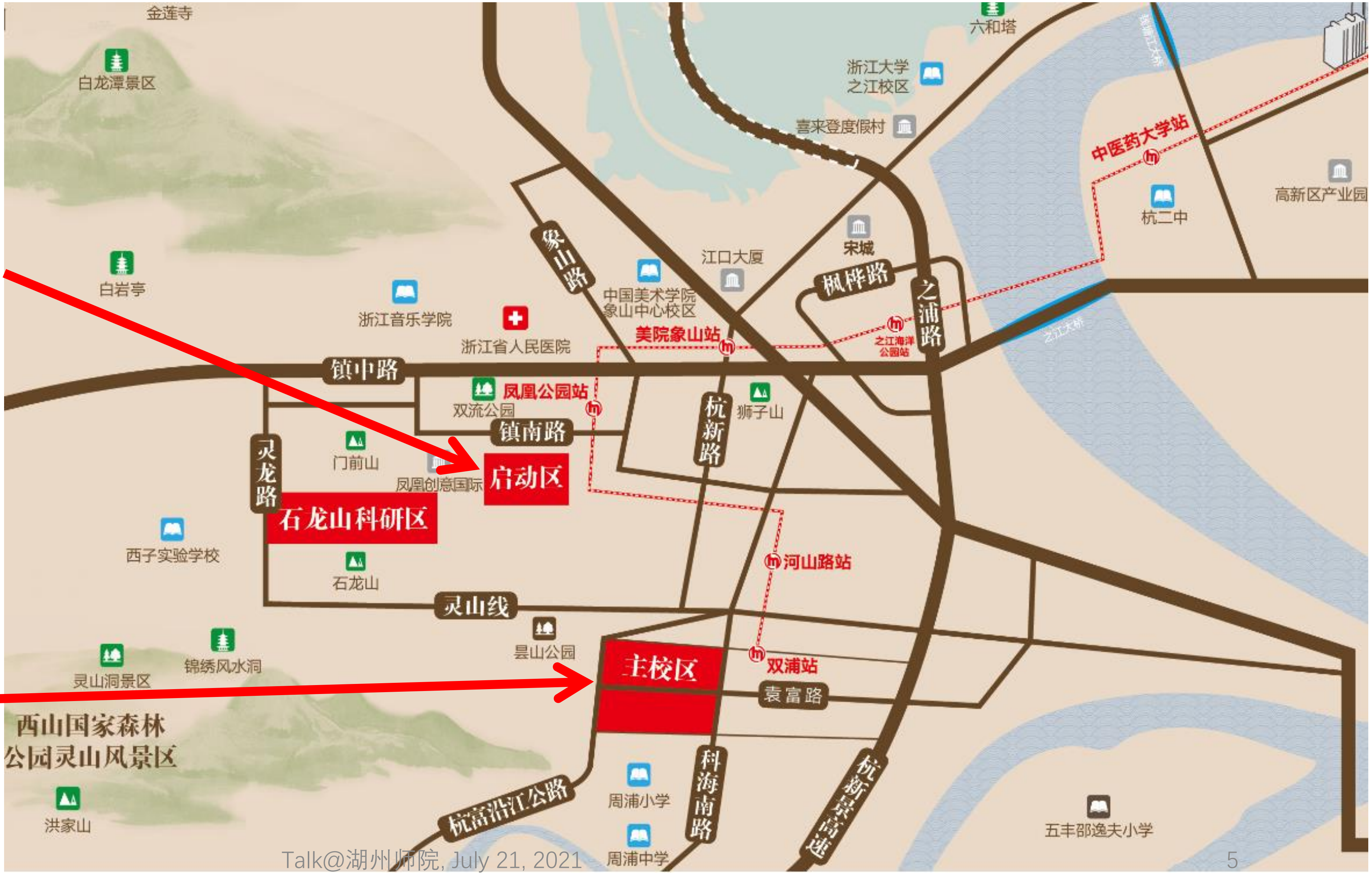

国科大杭高院数理学院一瞥

基础物理与数学科学学院（简称“数理学院”）是国科大杭州高等研究院下属二级学院。学院由**联合国教科文组织国际理论物理中心-亚太地区**和**中国科学院理论物理研究所**联合承办，学院秉承“科教融合、育人为本、开放合作、服务国家、提升杭州”的办学理念，与海内外一流高校、科研机构合作，目标建成国际一流的科学研究中心、国际化人才培养基地、开放型国际学术交流平台。

重大突破方向:

1. 量子宇宙物理
2. 太空推进和无托曳航天关键技术
3. 激光干涉测距系统关键技术

重点培育方向:

1. 应用数学与数学物理
2. 基础数学
3. 量子物相物理与应用基础物理
4. 量子生物物理与生命起源
5. 计算物理与数据科学及智能物理仿真

国科大杭高院数理学院一瞥

国科大杭州高等研究院 Hangzhou Institute For Advanced Study,UCAS

理论物理 — 招收（直）博士生、硕士生

吴岳良教授工作室	量子宇宙物理、宇宙起源和演化及引力波
蔡荣根教授工作室	引力波和黑洞物理与引力宇宙
耿朝强教授工作室	粒子物理和宇宙学

实验物理 — 招收专业硕士

徐溆岩教授工作室	引力波物理、太空推进理论和技术及仿真和实验测试技术
靳刚教授工作室	精密测量物理和激光干涉测距技术

国科大杭高院数理学院一瞥

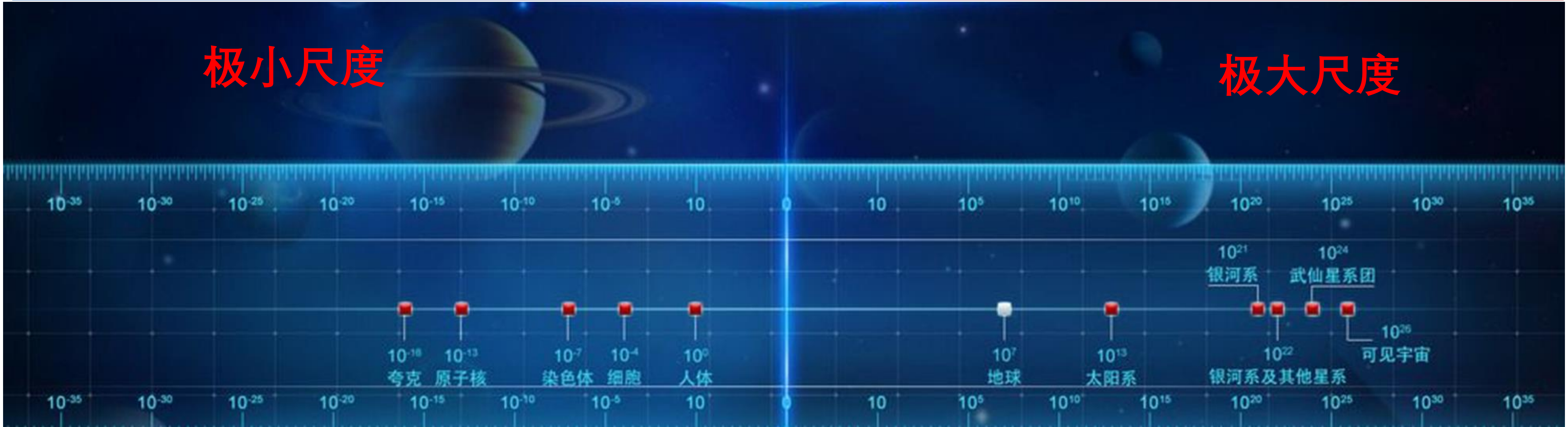

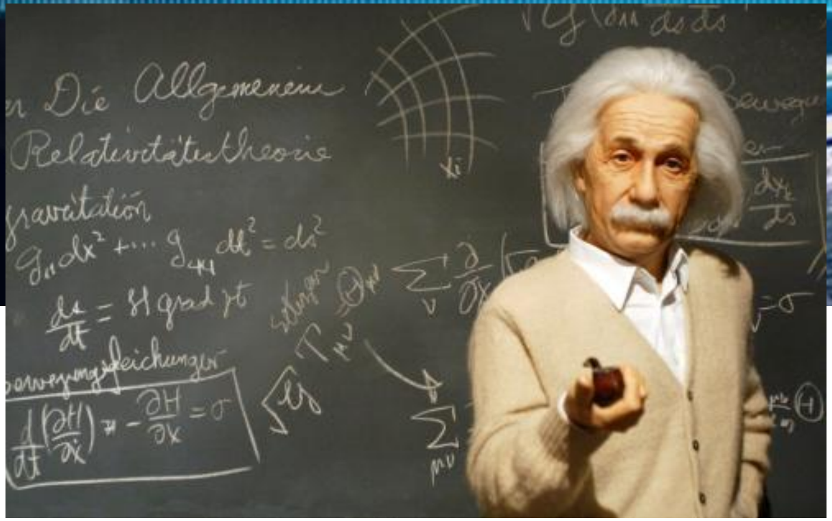

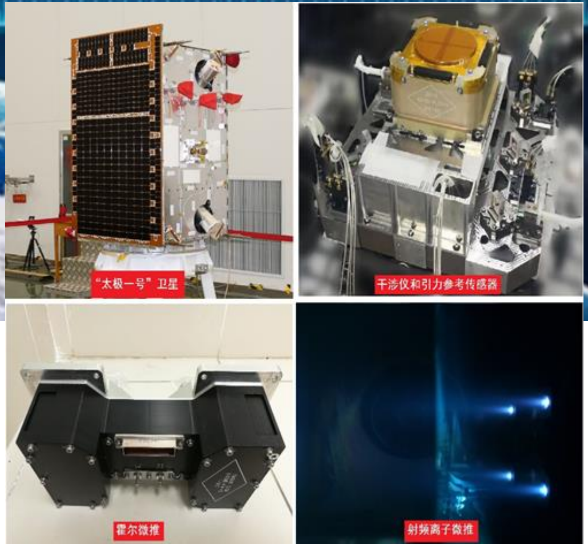


言归正传

NS $\sim 2.3\ M_{solar}$ has $n_{cent} \sim (5-7) n_0$
may contain quarks in some form.

G. Baym, et al., 1707.04966

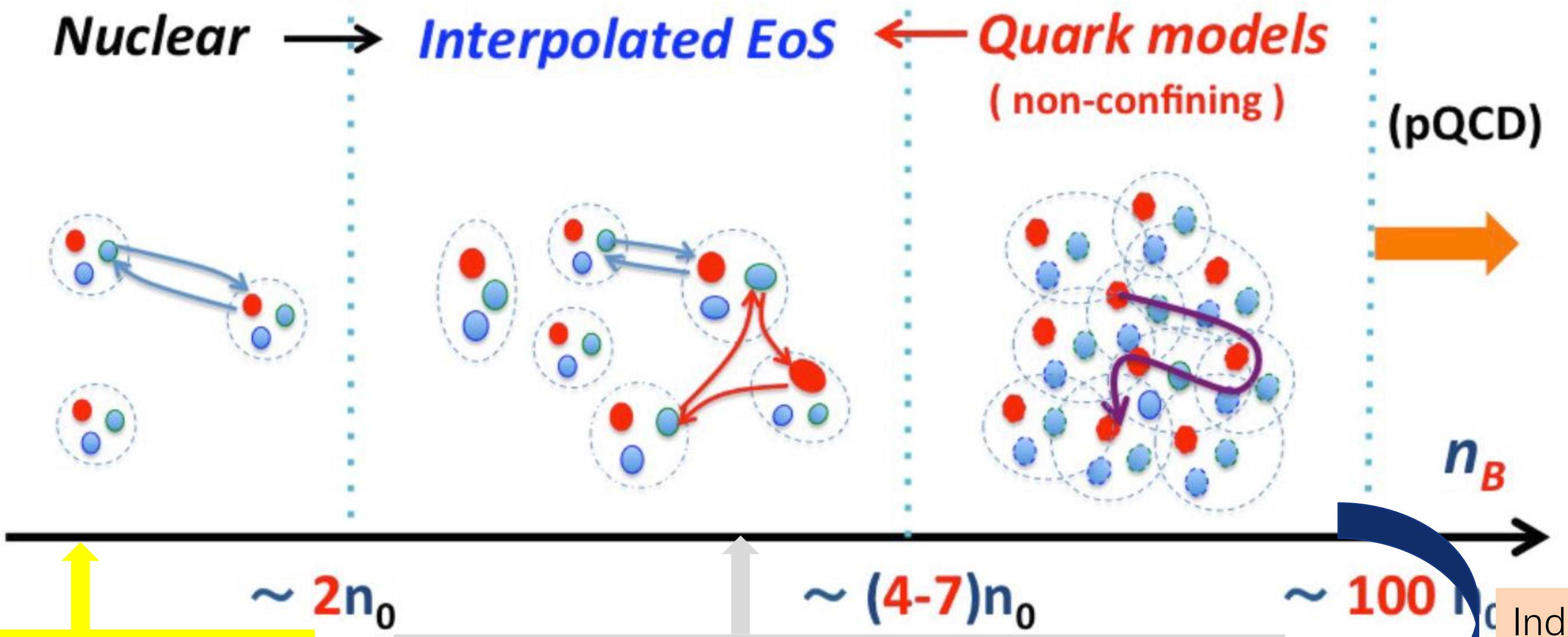

Terrestrial experiments on nucleon physics

- Cannot be accessed by terrestrial experiments, lattice QCD, fundamental QCD!
- Indirect information from astrophysics.

Indirect constraints on the model/EoS construction

- EoS of nuclear matter:

  At high density $\geq 2.0\, n_0$, mess.

  - What is the matter made of?
  - How to simulate the nuclear force?
  - Beyond mean field, SχEFT ……

- Cannot be accessed by lattice simulation (sign prob.)

  - Cannot be distinguished from QCD.

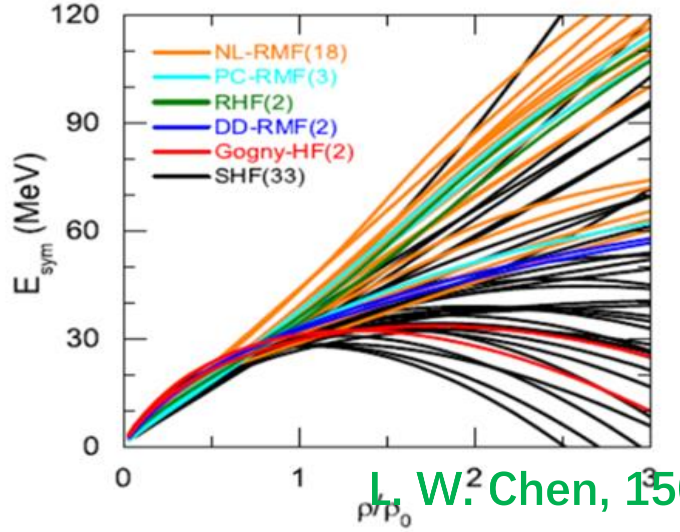

L. W. Chen, 1506.09057

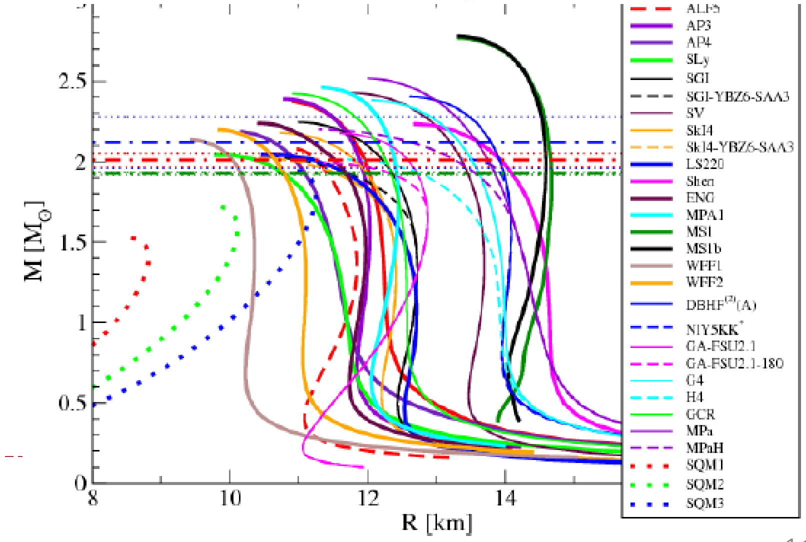

中子星的内部组成：

- Pure hadronic matter
- Quark matter
- Quark-hadron crossover
- ***Topology change***
- Strange matter
- ……

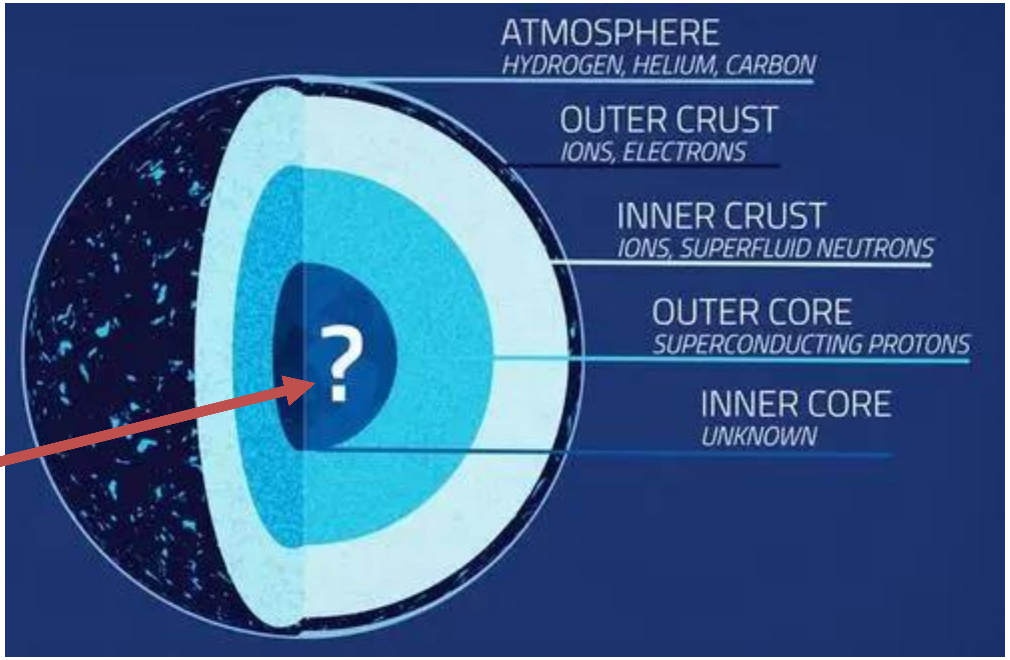

Selected for a Viewpoint in *Physics*
PRL **119,** 161101 (2017) PHYSICAL REVIEW LETTERS week ending 20 OCTOBER 2017

GW170817: Observation of Gravitational Waves from a Binary Neutron Star Inspiral

B. P. Abbott *et al.*[*]
(LIGO Scientific Collaboration and Virgo Collaboration)

(Received 26 September 2017; revised manuscript received 2 October 2017; published 16 October 2017)

On August 17, 2017 at 12:41:04 UTC the Advanced LIGO and Advanced Virgo gravitational-wave detectors made their first observation of a binary neutron star inspiral. The signal, GW170817, was detected with a combined signal-to-noise ratio of 32.4 and a false-alarm-rate estimate of less than one per 8.0×10^4 years. We infer the component masses of the binary to be between 0.86 and 2.26 $M_\odot$, in agreement with masses of known neutron stars. Restricting the component spins to the range inferred in binary neutron stars, we find the component masses to be in the range 1.17–1.60 $M_\odot$, with the total mass of the system $2.74^{+0.04}_{-0.01} M_\odot$. The source was localized within a sky region of 28 deg^2 (90% probability) and had a luminosity distance of 40^{+8}_{-14} Mpc, the closest and most precisely localized gravitational-wave signal yet. The association with the γ-ray burst GRB 170817A, detected by Fermi-GBM 1.7 s after the coalescence, corroborates the hypothesis of a neutron star merger and provides the first direct evidence of a link between these mergers and short γ-ray bursts. Subsequent identification of transient counterparts across the electromagnetic spectrum in the same location further supports the interpretation of this event as a neutron star merger. This unprecedented joint gravitational and electromagnetic observation provides insight into astrophysics, dense matter, gravitation, and cosmology.

DOI: 10.1103/PhysRevLett.119.161101

I. INTRODUCTION

On August 17, 2017, the LIGO-Virgo detector network observed a gravitational-wave signal from the inspiral of two low-mass compact objects consistent with a binary neutron star (BNS) merger. This discovery comes four decades after Hulse and Taylor discovered the first neutron star binary, PSR B1913+16 [1]. Observations of PSR B1913+16 found that its orbit was losing energy due to the emission of gravitational waves, providing the first indirect evidence of their existence [2]. As the orbit of a BNS system shrinks, the gravitational-wave luminosity increases, accelerating the inspiral. This process has long been predicted to produce a gravitational-wave signal observable by ground-based detectors [3–6] in the final minutes before the stars collide [7].

Since the Hulse-Taylor discovery, radio pulsar surveys have found several more BNS systems in our galaxy [8]. Understanding the orbital dynamics of these systems will observe between one BNS merger every few years to hundreds per year [14–21]. This detector network currently includes three Fabry-Perot-Michelson interferometers that measure spacetime strain induced by passing gravitational waves as a varying phase difference between laser light propagating in perpendicular arms: the two Advanced LIGO detectors (Hanford, WA and Livingston, LA) [22] and the Advanced Virgo detector (Cascina, Italy) [23].

Advanced LIGO's first observing run (O1), from September 12, 2015, to January 19, 2016, obtained 49 days of simultaneous observation time in two detectors. While two confirmed binary black hole (BBH) mergers were discovered [24–26], no detections or significant candidates had component masses lower than $5M_\odot$, placing a 90% credible upper limit of 12 600 $\mathrm{Gpc}^{-3}\,\mathrm{yr}^{-1}$ on the rate of BNS mergers [27] (credible intervals throughout this Letter contain 90% of the posterior probability unless noted otherwise). This measurement did not impinge on the range

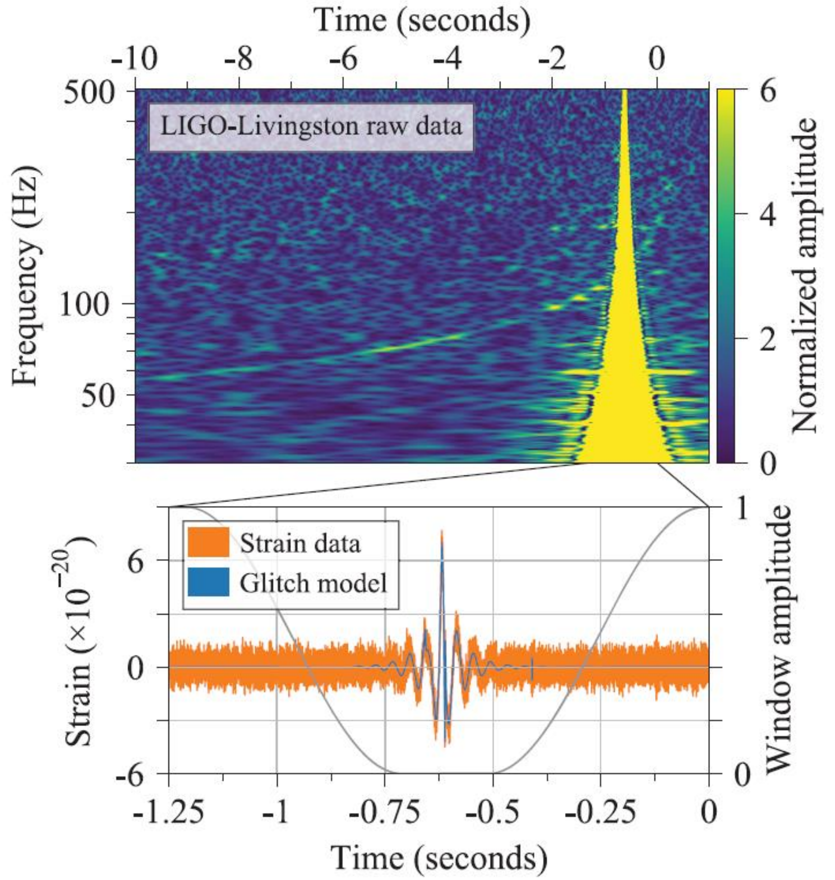

FIG. 2. Mitigation of the glitch in LIGO-Livingston data. Times are shown relative to August 17, 2017 12:41:04 UTC. *Top panel*: A time-frequency representation [65] of the raw LIGO-Livingston data used in the initial identification of GW170817 [76]. The coalescence time reported by the search is at time 0.4 s in this figure and the glitch occurs 1.1 s before this time. The time-frequency track of GW170817 is clearly visible despite the presence of the glitch. *Bottom panel*: The raw LIGO-Livingston

Science
AAAS

2017 BREAKTHROUGH *of the* YEAR

双中子星并合 GW20170817

- 天文学进入了多信使时代;
- 为研究高密度去物理提供了新的机遇

PRL 119, 161101 (2017) Selected for a Viewpoint in *Physics* PHYSICAL REVIEW LETTERS week ending 20 OCTOBER 2017

GW170817: Observation of Gravitational Waves from a Binary Neutron Star Inspiral

B. P. Abbott *et al.*[*]
(LIGO Scientific Collaboration and Virgo Collaboration)
(Received 26 September 2017; revised manuscript received 2 October 2017; published 16 October 2017)

- S/N = 33.0 (signal to noise ratio)
  - Assumption/setup of data analysis :
    - NS is not rotating rapidly like BH
    - Using the EM counterpart SSS17a/AT2017gfo for the source localization
    - Using distance indicated by the red-shift of the host galaxy NGC 4993
- Chirp mass : $\frac{(m_1 m_2)^{3/5}}{(m_1+m_2)^{1/5}} = 1.186^{+0.001}_{-0.001} M_{\odot}$
  - Total mass : $2.74 M_{\odot}$ (1%)
  - Mass ratio : $m_1/m_2 = 0.7 - 1.0$
    - **Primary mass (m1) : $1.46^{+0.12}_{-0.10} M_{\odot}$**
    - **Secondary (m2) : $1.27^{+0.09}_{-0.09} M_{\odot}$**
- Luminosity distance to the source : 40^{+10}_{-10} Mpc

90% C.L

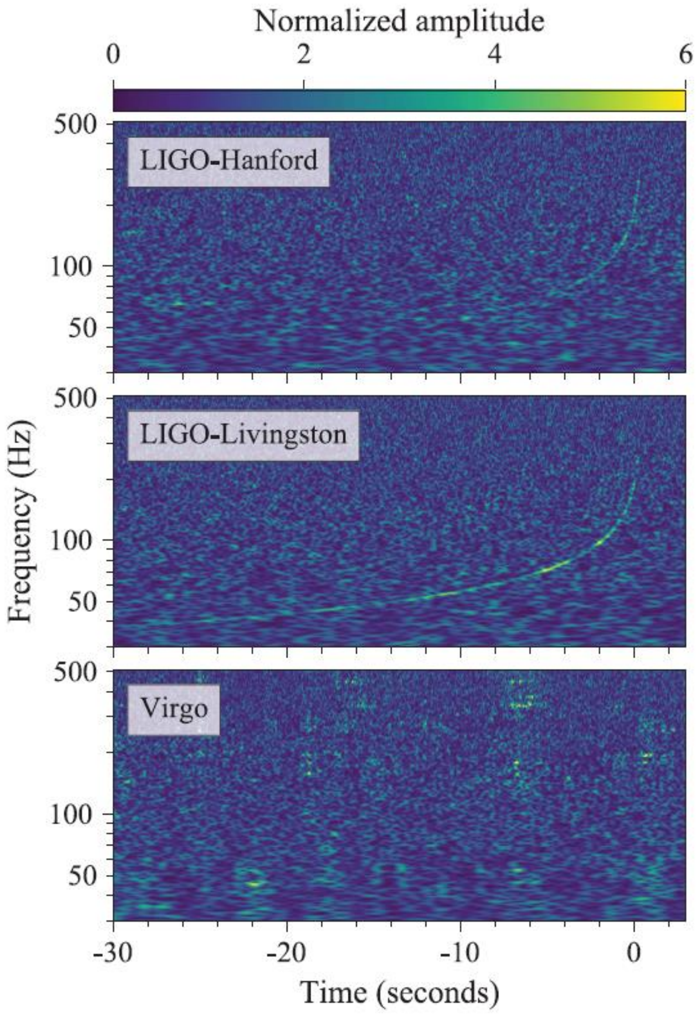

FIG. 1. Time-frequency representations [65] of data containing the gravitational-wave event GW170817, observed by the LIGO-Hanford (top), LIGO-Livingston (middle), and Virgo (bottom) detectors. Times are shown relative to August 17, 2017 12:41:04 UTC. The amplitude scale in each detector is normalized to that detector's noise amplitude spectral density. In the LIGO data, independently observable noise sources and a glitch that occurred in the LIGO-Livingston detector have been subtracted, as described in the text. This noise mitigation is the same as that

Tolman-Oppenheimer-Volkoff (TOV) 方程

国科大杭州高等研究院
Hangzhou Institute For Advanced Study,UCAS

$$R^{\mu\nu}-\frac{1}{2}g^{\mu\nu}R=-8\pi T^{\mu\nu}$$

$$ds^2=e^{2\nu}dt^2-e^{2\lambda}dr^2-r^2(d\theta^2+sin^2\theta d\varphi^2)$$

$$T^{\mu\nu}=u^\mu u^\nu(\varepsilon+p)-g^{\mu\nu}p$$

$$\frac{dm}{dr}=4\pi r^2\varepsilon$$

$$\frac{dp}{dr}=-\frac{(m+4\pi r^3 p)(\varepsilon+p)}{r^2(1-2m/r)}$$

对中子星结构的认识主要来自于质量-半径关系的确定

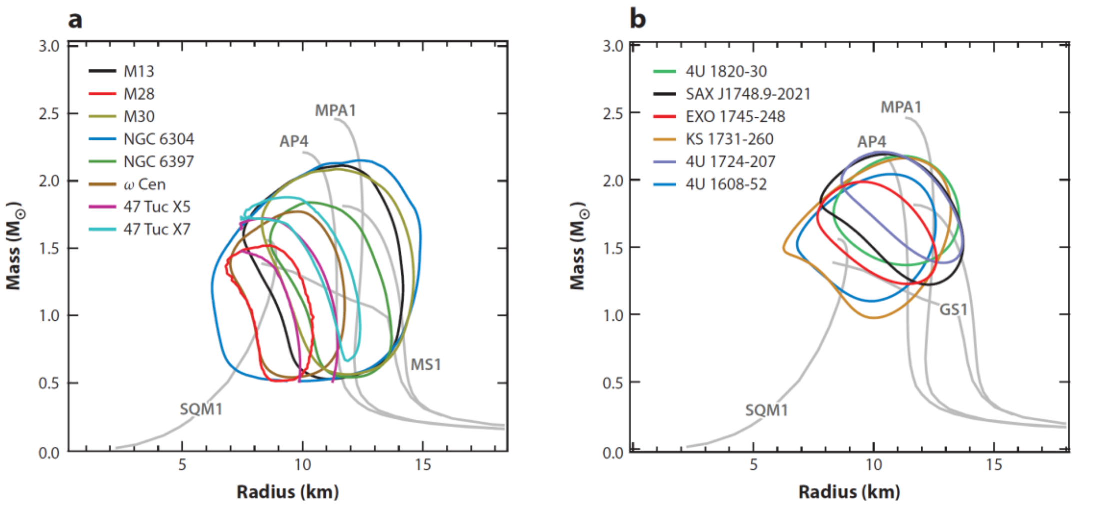

Figure 4

The combined constraints at the 68% C.L. over the neutron-star mass and radius obtained from (*a*) all neutron stars in low-mass X-ray binaries during quiescence and (*b*) all neutron stars with thermonuclear bursts. The light gray lines show mass relations corresponding to a few representative EoSs (see Section 4.1 and **Figure 7** for detailed descriptions and the naming conventions for all equations of state).

Feryal Özel, Paulo Freire, 1603.02698

- Tidal deformability(GW170817):

$\Lambda_{1.4} < 800$

$$\tilde{\Lambda} = 300^{+420}_{-230} \rightarrow \tilde{\Lambda} = 190^{+390}_{-120}$$

$$R = 11.9^{+1.4}_{-1.4}\ km$$

C. Y. Tsang, *et al.*, 1807.06571

- Pressure:

$$P(2n_0) = 3.5^{+2.7}_{-1.7} \times 10^{34} \mathrm{dyn/cm^2},$$
$$P(6n_0) = 9.0^{+7.9}_{-2.6} \times 10^{34} \mathrm{dyn/cm^2}.$$

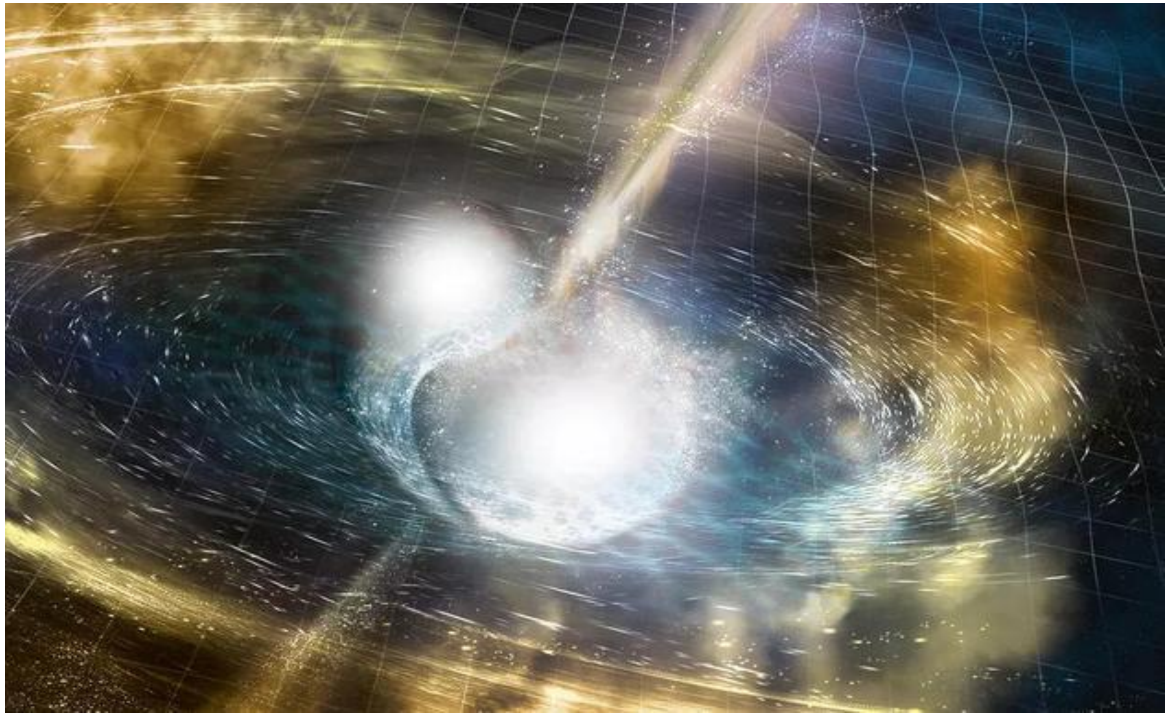

- Massive neutron stars:

$(1.97 \pm 0.04) M_\odot$ *Nature, 467(2010),1081.*

$(2.01 \pm 0.04) M_\odot$ *Science, 340(2013), 448.*

$(2.14^{+0.10}_{-0.09}) M_\odot$ *Nature Astronomy, 4 (2020)72.*

$\leq 10 n_0$

THE ASTROPHYSICAL JOURNAL LETTERS, 892:L3 (24pp), 2020 March 20 https://doi.org/10.3847/2041-8213/ab75f5

GW190425: Observation of a Compact Binary Coalescence with Total Mass $\sim 3.4 M_{\odot}$

Table 1
Source Properties for GW190425

	Low-spin Prior ($\chi < 0.05$)	High-spin Prior ($\chi < 0.89$)
Primary mass m_1	1.60–1.87 $M_{\odot}$	1.61–2.52 $M_{\odot}$
Secondary mass m_2	1.46–1.69 $M_{\odot}$	1.12–1.68 $M_{\odot}$
Chirp mass $\mathcal{M}$	$1.44^{+0.02}_{-0.02}$ $M_{\odot}$	$1.44^{+0.02}_{-0.02}$ $M_{\odot}$
Detector-frame chirp mass	$1.4868^{+0.0003}_{-0.0003}$ $M_{\odot}$	$1.4873^{+0.0008}_{-0.0006}$ $M_{\odot}$
Mass ratio m_2/m_1	0.8 – 1.0	0.4 – 1.0
Total mass $m_{\rm tot}$	$3.3^{+0.1}_{-0.1}$ $M_{\odot}$	$3.4^{+0.3}_{-0.1}$ $M_{\odot}$
Effective inspiral spin parameter $\chi_{\rm eff}$	$0.012^{+0.01}_{-0.01}$	$0.058^{+0.11}_{-0.05}$
Luminosity distance $D_{\rm L}$	159^{+69}_{-72} Mpc	159^{+69}_{-71} Mpc
Combined dimensionless tidal deformability $\tilde{\Lambda}$	$\leqslant 600$	$\leqslant 1100$

Note. We give ranges encompassing the 90% credible intervals for the PhenomPv2NRT model; in Appendix D we demonstrate these results are robust to systematic uncertainty in the waveform. Mass values are quoted in the frame of the source, accounting for uncertainty in the source redshift. For the primary mass we give the 0%–90% interval, while for the secondary mass and mass ratio we give the 10%–100% interval: the uncertainty on the luminosity distance means that there is no well-defined equal-mass bound for GW190425. The quoted 90% upper limits for $\tilde{\Lambda}$ are obtained by reweighting its posterior distribution as detailed in Appendix F.1.

The Astrophysical Journal Letters, 896:L44 (20pp), 2020 June 20
https://doi.org/10.3847/2041-8213/ab960f

GW190814: Gravitational Waves from the Coalescence of a 23 Solar Mass Black Hole with a 2.6 Solar Mass Compact Object

Table 1
Source Properties of GW190814: We Report the Median Values Along with the Symmetric 90% Credible Intervals for the SEOBNRv4PHM (EOBNR PHM) and IMRPhenomPv3HM (Phenom PHM) Waveform Models

	EOBNR PHM	Phenom PHM	Combined
Primary mass $m_1/M_\odot$	$23.2^{+1.0}_{-0.9}$	$23.2^{+1.3}_{-1.1}$	$23.2^{+1.1}_{-1.0}$
Secondary mass $m_2/M_\odot$	$2.59^{+0.08}_{-0.08}$	$2.58^{+0.09}_{-0.10}$	$2.59^{+0.08}_{-0.09}$
Mass ratio q	$0.112^{+0.008}_{-0.008}$	$0.111^{+0.009}_{-0.010}$	$0.112^{+0.008}_{-0.009}$
Chirp mass $\mathcal{M}/M_\odot$	$6.10^{+0.06}_{-0.05}$	$6.08^{+0.06}_{-0.05}$	$6.09^{+0.06}_{-0.06}$
Total mass $M/M_\odot$	$25.8^{+0.9}_{-0.8}$	$25.8^{+1.2}_{-1.0}$	$25.8^{+1.0}_{-0.9}$
Final mass $M_f/M_\odot$	$25.6^{+1.0}_{-0.8}$	$25.5^{+1.2}_{-1.0}$	$25.6^{+1.1}_{-0.9}$
Upper bound on primary spin magnitude χ_1	0.06	0.08	0.07
Effective inspiral spin parameter χ_{eff}	$0.001^{+0.059}_{-0.056}$	$-0.005^{+0.061}_{-0.065}$	$-0.002^{+0.060}_{-0.061}$
Upper bound on effective precession parameter χ_p	0.07	0.07	0.07
Final spin χ_f	$0.28^{+0.02}_{-0.02}$	$0.28^{+0.02}_{-0.03}$	$0.28^{+0.02}_{-0.02}$
Luminosity distance D_L/Mpc	235^{+40}_{-45}	249^{+39}_{-43}	241^{+41}_{-45}
Source redshift z	$0.051^{+0.008}_{-0.009}$	$0.054^{+0.008}_{-0.009}$	$0.053^{+0.009}_{-0.010}$
Inclination angle Θ/rad	$0.9^{+0.3}_{-0.2}$	$0.8^{+0.2}_{-0.2}$	$0.8^{+0.3}_{-0.2}$

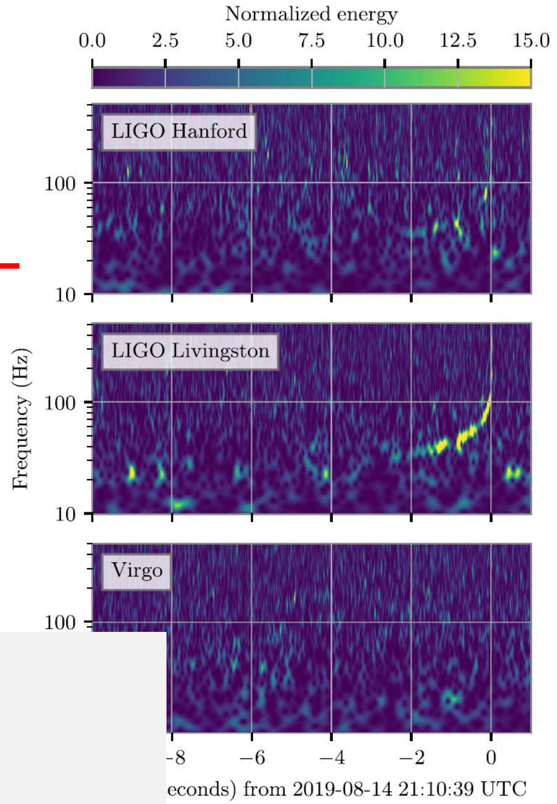

- GW190814, $\sim 2.59^{+0.08}_{-0.09} M_\odot$,

A slow rotating NS? A very rapidly rotation NS? Challenge on EoS.

THE ASTROPHYSICAL JOURNAL LETTERS, 915:L5 (24pp), 2021 July 1 https://doi.org/10.3847/2041-8213/ac082e

Observation of Gravitational Waves from Two Neutron Star–Black Hole Coalescences

Table 2
Source Properties of GW200105 and GW200115

	GW200105		GW200115	
	Low Spin ($\chi_2 < 0.05$)	High Spin ($\chi_2 < 0.99$)	Low Spin ($\chi_2 < 0.05$)	High Spin ($\chi_2 < 0.99$)
Primary mass $m_1/M_\odot$	$8.9^{+1.1}_{-1.3}$	$8.9^{+1.2}_{-1.5}$	$5.9^{+1.4}_{-2.1}$	$5.7^{+1.8}_{-2.1}$
Secondary mass $m_2/M_\odot$	$1.9^{+0.2}_{-0.2}$	$1.9^{+0.3}_{-0.2}$	$1.4^{+0.6}_{-0.2}$	$1.5^{+0.7}_{-0.3}$
Mass ratio q	$0.21^{+0.06}_{-0.04}$	$0.22^{+0.08}_{-0.04}$	$0.24^{+0.31}_{-0.08}$	$0.26^{+0.35}_{-0.10}$
Total mass $M/M_\odot$	$10.8^{+0.9}_{-1.0}$	$10.9^{+1.1}$ [illegible]	$7.3^{+1.2}$ [illegible]	$7.1^{+1.5}_{-1.4}$
Chirp mass $\mathcal{M}/M_\odot$	$3.41^{+0.08}_{-0.07}$	[illegible]	[illegible]	[illegible]$2^{+0.05}_{-0.07}$
Detector-frame chirp mass $(1 + z)\mathcal{M}/M_\odot$	$3.619^{+0.0}_{-0.0}$[illegible]	[illegible]	[illegible]	[illegible]$9^{+0.007}_{-0.007}$
Primary spin magnitude χ_1	$0.09^{+0.1}_{-0.0}$[illegible]	[illegible]	[illegible]	[illegible]$3^{+0.48}_{-0.29}$
Effective inspiral spin parameter $\chi_{\rm eff}$	$-0.01^{+0.}_{-0.}$[illegible]	[illegible]	[illegible]	[illegible]$19^{+0.23}_{-0.35}$
Effective precession spin parameter χ_p	$0.07^{+0.1}_{-0.0}$[illegible]	[illegible]	[illegible]	[illegible]$1^{+0.30}_{-0.17}$
Luminosity distance $D_{\rm L}$/Mpc	280^{+110}_{-110}	[illegible]	[illegible]	[illegible]0^{+150}_{-100}
Source redshift z	$0.06^{+0.0}_{-0.0}$[illegible]	[illegible]	[illegible]	[illegible]$7^{+0.03}_{-0.02}$

Note. We report the median values with 90% credible intervals. Paran

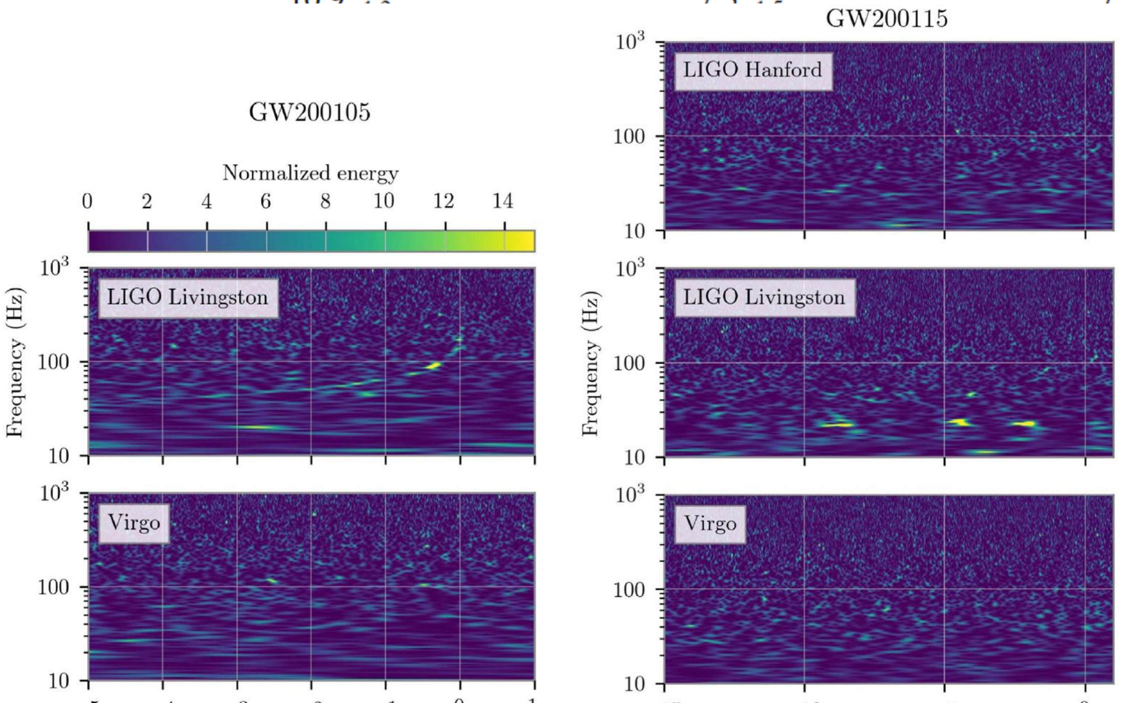

PHYSICAL REVIEW LETTERS **120,** 172703 (2018)

Editors' Suggestion | Featured in Physics

Gravitational-Wave Constraints on the Neutron-Star-Matter Equation of State

Eemeli Annala,[1] Tyler Gorda,[1] Aleksi Kurkela,[2] and Aleksi Vuorinen[1]

[1]*Department of Physics and Helsinki Institute of Physics, P.O. Box 64, FI-00014 University of Helsinki, Finland*

[2]*Theoretical Physics Department, CERN, Geneva CH-1211, Switzerland*

Stavange

eived 6 Fe

Impact of $\tilde{\Lambda} < 800$ on NS radius & EOS

- **$\Lambda_{1.4} \lesssim 800$: in terms of NS radius $10 \lesssim R_{1.4M_\odot} \lesssim 13.5$ km for an EOS**
  - connects to the NNLO pQCD (Kurkela et al. 2010) and chiral EFT (Hebeler et al. 2013)
  - causality $c_s < c$ and $M_{\mathrm{EOS,max}} \gtrsim 2M_\odot$ constraints in the intermediate region

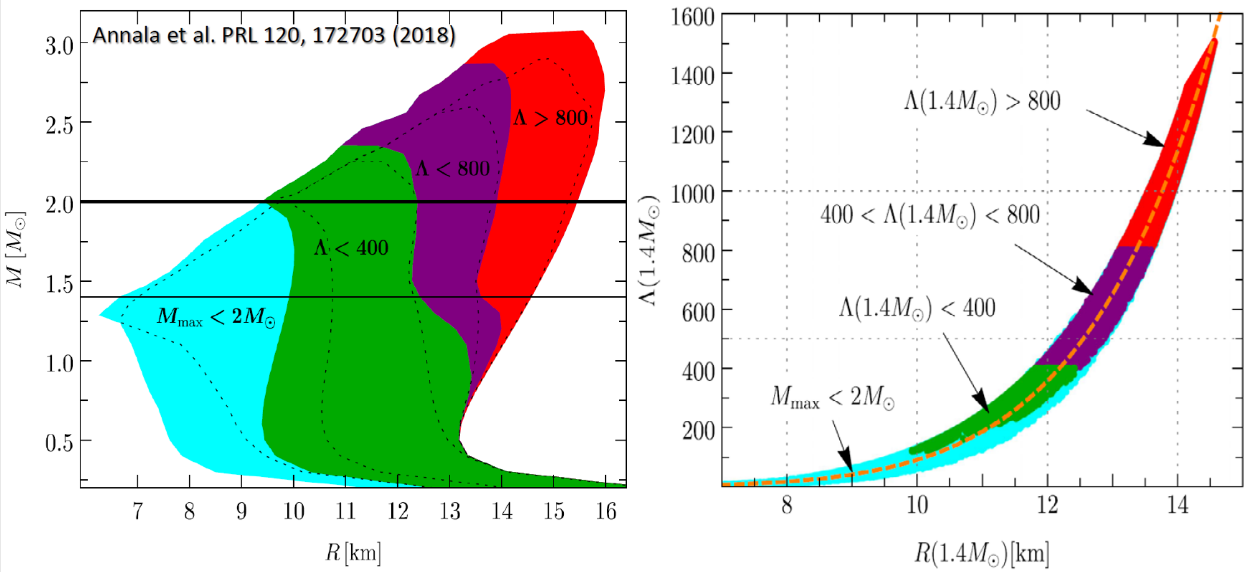

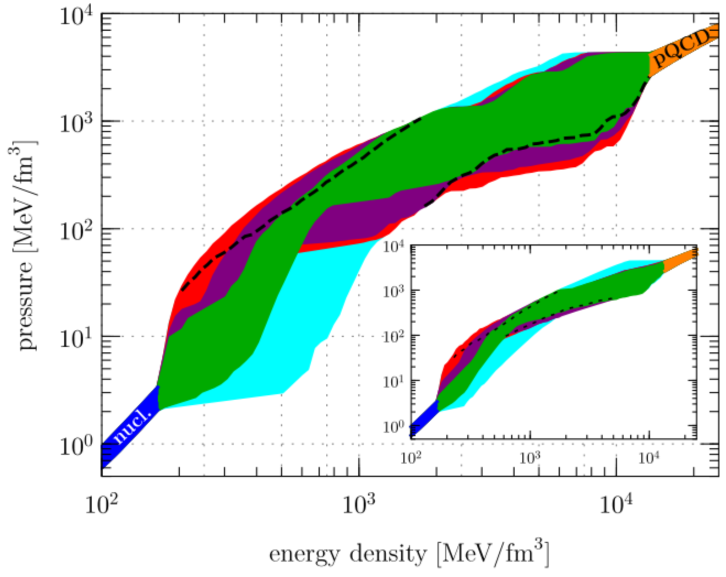

FIG. 3. Our ensemble of EOSs shown in the form of ϵ vs p. The color coding follows that of the previous figures, with the addition of a blue region indicating the nuclear EOSs and an orange region indicating the PQCD EOS. The black dashed lines indicate where the upper and lower edges become truncated with a further restriction of $M_{\max} < 2.16\,M_\odot$ (see Refs. [25–27]). Inset: The same function constructed with tritropic interpolating functions only.

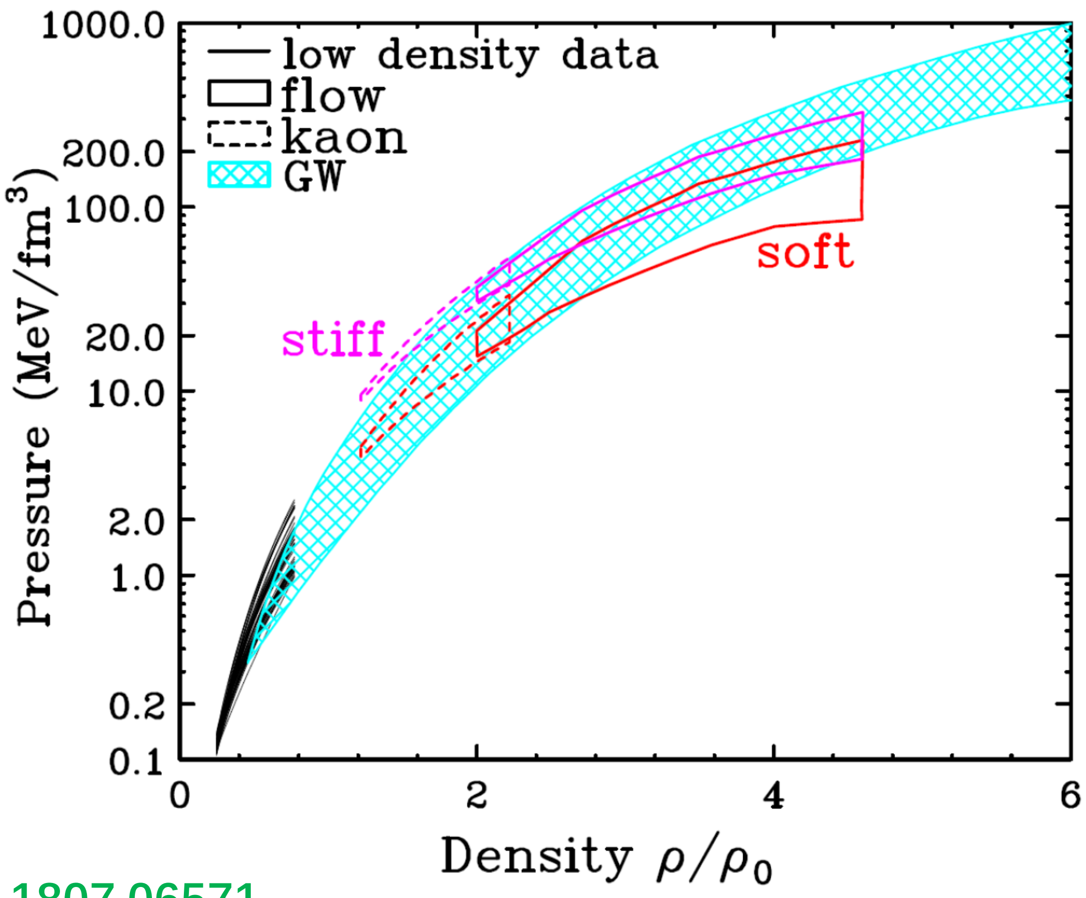

C. Y. Tsang, *et al.*, 1807.06571

Standard Scenario

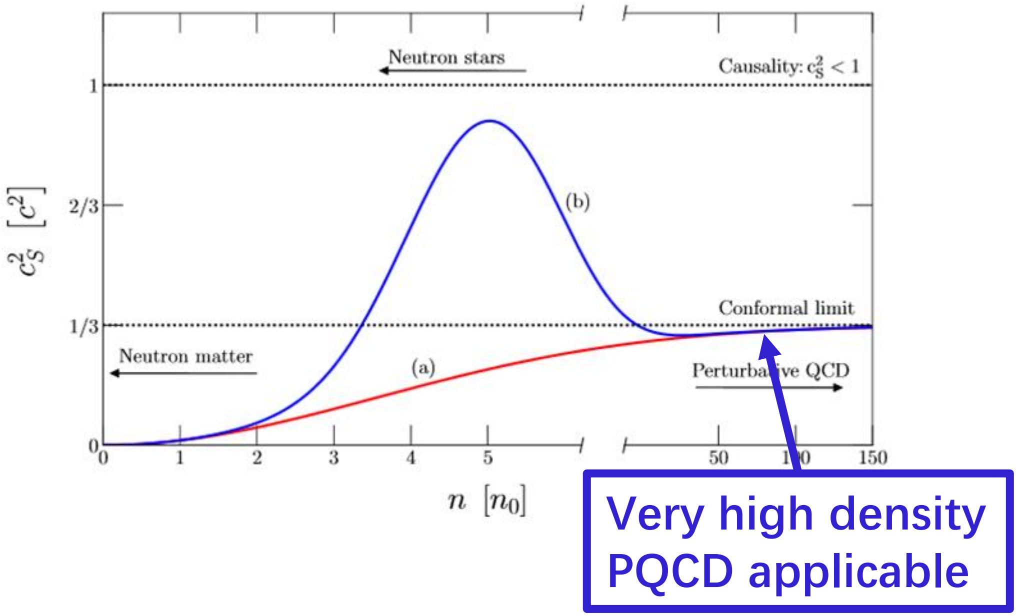

?

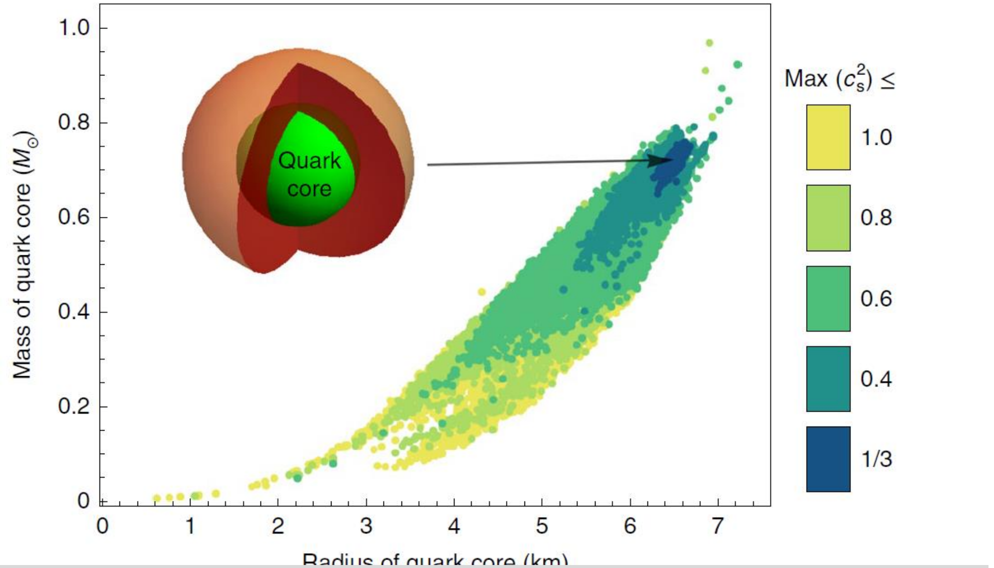

Polytropic index $\gamma = d(\ln p)/d(\ln \epsilon) < 2.3 \rightarrow 1$

We found that the conformal limit of $c_S^2 \leqslant 1/3$ is in tension with current nuclear physics constraints and observations of two-solar-mass NSs, in accordance with the findings of Bedaque & Steiner (2015). If the conformal limit was found to hold at all densities, this would imply that nuclear physics models break down below $2n_0$.

S. Reddy et al, 2018

for the presence of quark-matter cores. For the heaviest reliably observed neutron stars[5,6] with mass $M \approx 2M_\odot$, the presence of quark matter is found to be linked to the behaviour of the speed of sound c_s in strongly interacting matter. If the conformal bound $c_s^2 \leq 1/3$ (ref. [7]) is not strongly violated, massive neutron stars are predicted to have sizable quark-matter cores. This finding has important implications for the phe-

E. Annala, et al, Nature Physics 2020

典型模型：Pure hadronic matter

国科大杭州高等研究院
Hangzhou Institute For Advanced Study,UCAS

$$\mathcal{L} = \bar{\psi}\left(\gamma\left(i\partial - g_\omega \omega - g_\rho \vec{\rho}\vec{\tau} - eA\right) - m - g_\sigma \sigma\right)\psi$$
$$+ \frac{1}{2}(\partial\sigma)^2 - U(\sigma) - \frac{1}{4}\Omega_{\mu\nu}\Omega^{\mu\nu} + \frac{1}{2}m_\omega^2\omega^2$$
$$- \frac{1}{4}\vec{\mathrm{R}}_{\mu\nu}\vec{\mathrm{R}}^{\mu\nu} + \frac{1}{2}m_\rho^2\vec{\rho}^2$$
$$- \frac{1}{4}\mathrm{F}_{\mu\nu}\mathrm{F}^{\mu\nu},$$

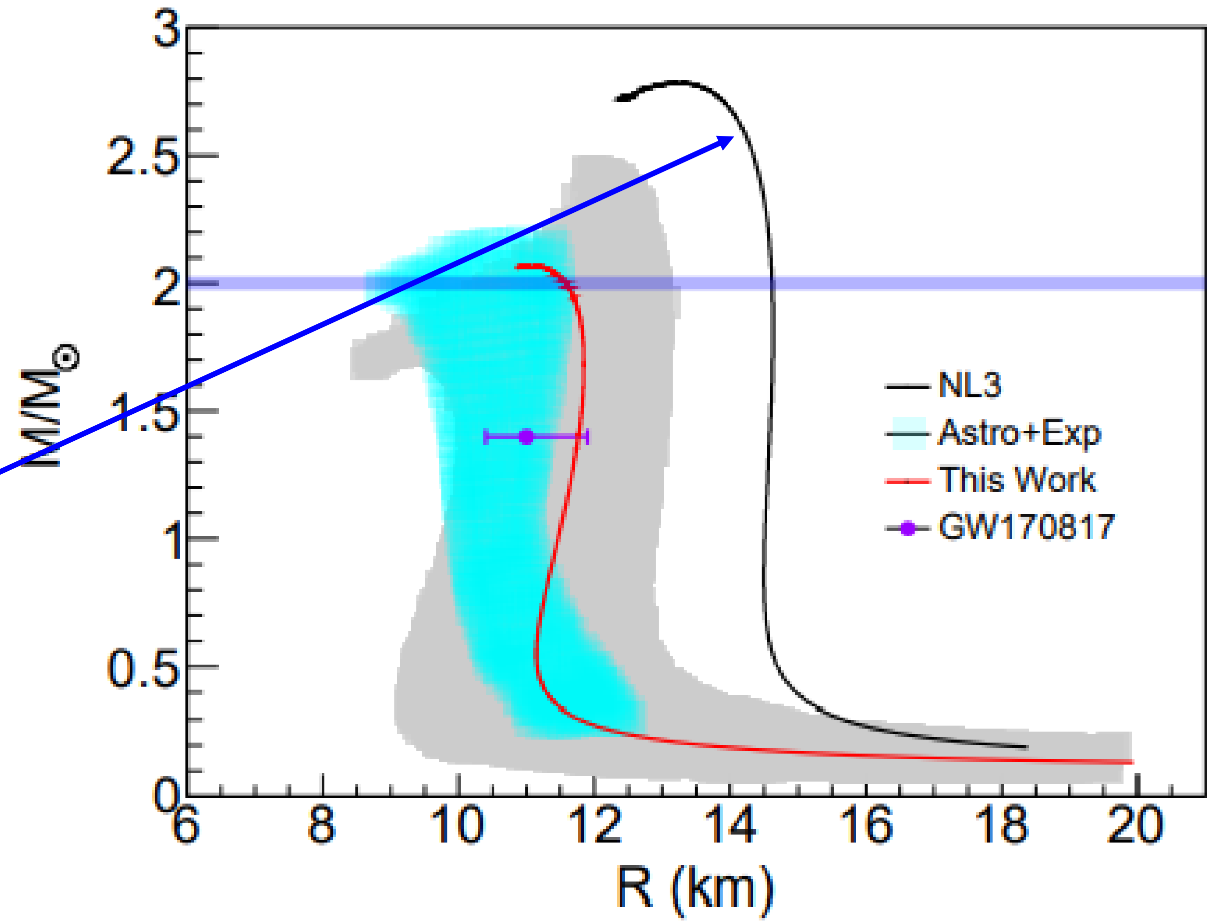

典型模型：Quark matter

Mexwell construction

$$\mathcal{E}(p) = \begin{cases} \mathcal{E}_{\mathrm{APR+MDI}}(p), & p < p_{\mathrm{tr}} \\ \mathcal{E}(p_{\mathrm{tr}}) + \Delta\mathcal{E} + (p - p_{\mathrm{tr}})\, c_{\mathrm{s}}^{-2}, & p \geq p_{\mathrm{tr}} \end{cases}$$

J.E. Christian, et al., EPJA54, 28 (2018);
G. Montana, et al., PRD 99, 103009 (2019)

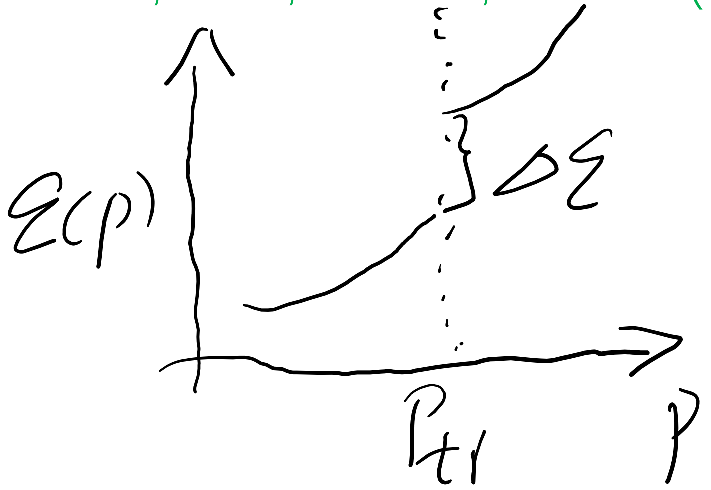

Gibbs construction

$$\mathcal{E}(p) = \begin{cases} \mathcal{E}_{\mathrm{APR+MDI}}(p), & p \leq p_{\mathrm{tr}} \\ \Lambda p^{1/\Gamma} + p\,(\Gamma - 1)^{-1}, & p_{\mathrm{tr}} \leq p \leq p_{\mathrm{css}} \\ \mathcal{E}(p_{\mathrm{css}}) + (p - p_{\mathrm{css}})\, c_{\mathrm{s}}^{-2}, & p \geq p_{\mathrm{css}}. \end{cases}$$

A. Bhattacharyya, et al., JPG37, 025201 (2010);
B. T. Endo, et al., hep-ph/0502216

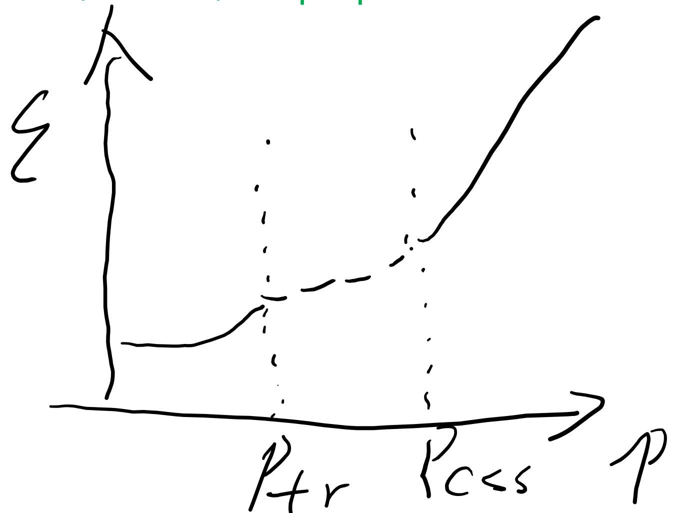

典型模型：

- Quark-hadron crossover

$$P(\mu) = S(\mu)P_q(\mu) + (1 - S(\mu))P_h(\mu)$$

$$P_q = \frac{N_f}{4\pi^2}\left(\frac{\mu}{3}\right)^4\left(1 - \frac{2\alpha_s}{\pi}\right)$$

- Strange matter

$$\mathcal{L}_\phi = g_{Y,\phi}\bar{\psi}_Y(\gamma^\mu\phi_\mu)\psi_Y + \frac{1}{2}m_\phi^2\phi_\mu\phi^\mu - \frac{1}{4}\Phi^{\mu\nu}\Phi_{\mu\nu}$$

$$\mathcal{L}_{\omega\rho} = \Lambda_{\omega\rho}(g_\rho^2\vec{\rho^\mu}\cdot\vec{\rho_\mu})(g_\omega^2\omega^\mu\omega_\mu);$$

典型模型：Quarkyonic matter

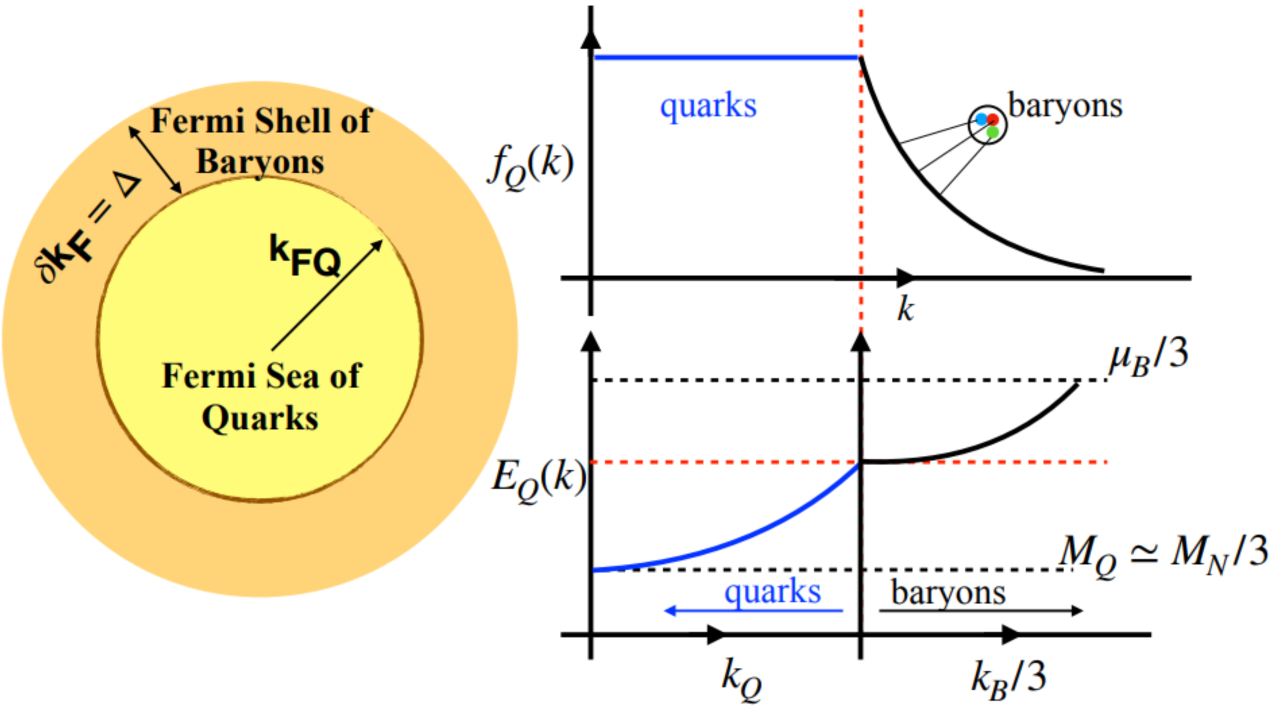

FIG. 1. The schematic shows the distribution of momentum and energy of quarks and baryons. The diffuse distribution of quarks in the right upper graph indicates they are confined inside baryons.

Basic assumption:

At large Fermi energy, the degrees of freedom inside the Fermi sea may be treated as quarks, confining forces remain important only near the Fermi surface. Nucleons emerge through correlations between quarks at the surface of the quark Fermi sea.

$$\epsilon(n_B) = 2\int_{N_c k_{\rm FQ}}^{k_{\rm FB}} \frac{d^3k}{(2\pi)^3}\sqrt{k^2+M_n^2} + V_n(n_n)$$
$$+ \sum_{i=u,d} N_c \int_0^{k_{\rm Fi}} \frac{d^3k}{(2\pi)^3}\sqrt{k^2+M_q^2}\,,$$

Larry McLerran and S. Reddy, 1811.12503

The pseudoconformal structure of dense nuclear matter

- ***Finite nuclei as well as infinite nuclear matter*** can be fairly accurately accessed by ***nuclear EFTs***, ``pionless or pionful, (*s*EFT)" anchored on relevant symmetries and invariances .

- *s*EFTs, as befits their premise, are expected to ***break down at some high density*** (and low temperature) relevant to, say, the interior of massive stars.

E.g, In sEFT, the power counting in density is $O(k_F^q)$. For the normal nuclear matter, the expansion requires going to $\sim q = 5$.

J. W. Holt, M. Rho and W.Weise, 1411.6681

Our strategy: Construct "Generalized" nuclear EFT (GnEFT) while capturing fully what *s*EFT successfully does up to n_0, can be extrapolated up to a density where *s*EFT is presumed to break down.

The pseudoconformal structure of dense nuclear matter

GnEFT = *s*EFT + ρ and ω + scalar meson $f_0(500)$

Hidden local symmetry (→ ρ and ω)

Dilaton/NGB of hidden scale symmetry (→ scalar meson $f_0(500)$)

- Not visible in the matter-free vacuum.
- *Get un-hidden by strong nonperturbative nuclear correlations, as nuclear matter is highly compressed.*

■ Hidden topology in QCD

- The microscopic degrees of QCD – quark and gluon – enters the system rephrased using Cheshire Cat Principle

YLM & M. Rho, *PPNP* 20';
W. G. Paeng, et al, *PRD* 17'.

Topology change and quark-hadron continuity

国科大杭州高等研究院
Hangzhou Institute For Advanced Study,UCAS

In large N_c limit, baryon in QCD goes to skyrmion. Witten 79'

$$\mathcal{L} = \frac{f_\pi^2}{4}\mathrm{Tr}\left(\partial_\mu U^\dagger \partial^\mu U\right) + \frac{1}{32e^2}\mathrm{Tr}\left[U^\dagger\partial_\mu U, U^\dagger\partial_\nu U\right]^2$$

f_π : pion decay constant

e : Skyrme parameter

Topological soliton

winding number = baryon number

$$B_\mu = \frac{1}{24\pi^2}\epsilon_{\mu\nu\alpha\beta}\mathrm{Tr}\left(U^\dagger\partial_\nu U U^\dagger\partial_\alpha U U^\dagger\partial_\beta U\right)$$

T. R. Skyrme, 1960

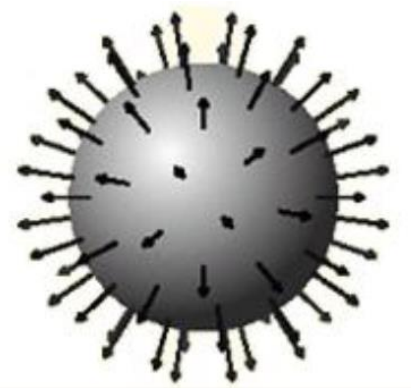

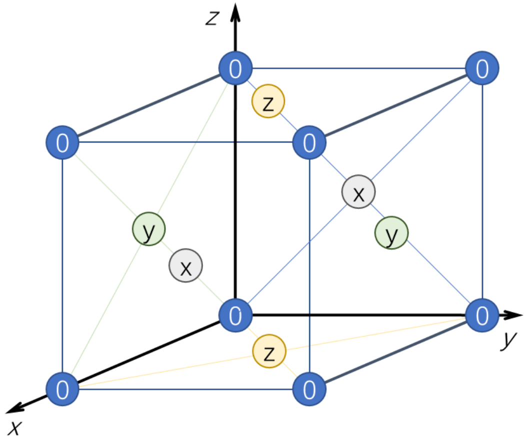

Baryonic interactions in all regimes of density, upto that relevant to the core of CSs, can be accessed.

Topology change and quark-hadron continuity

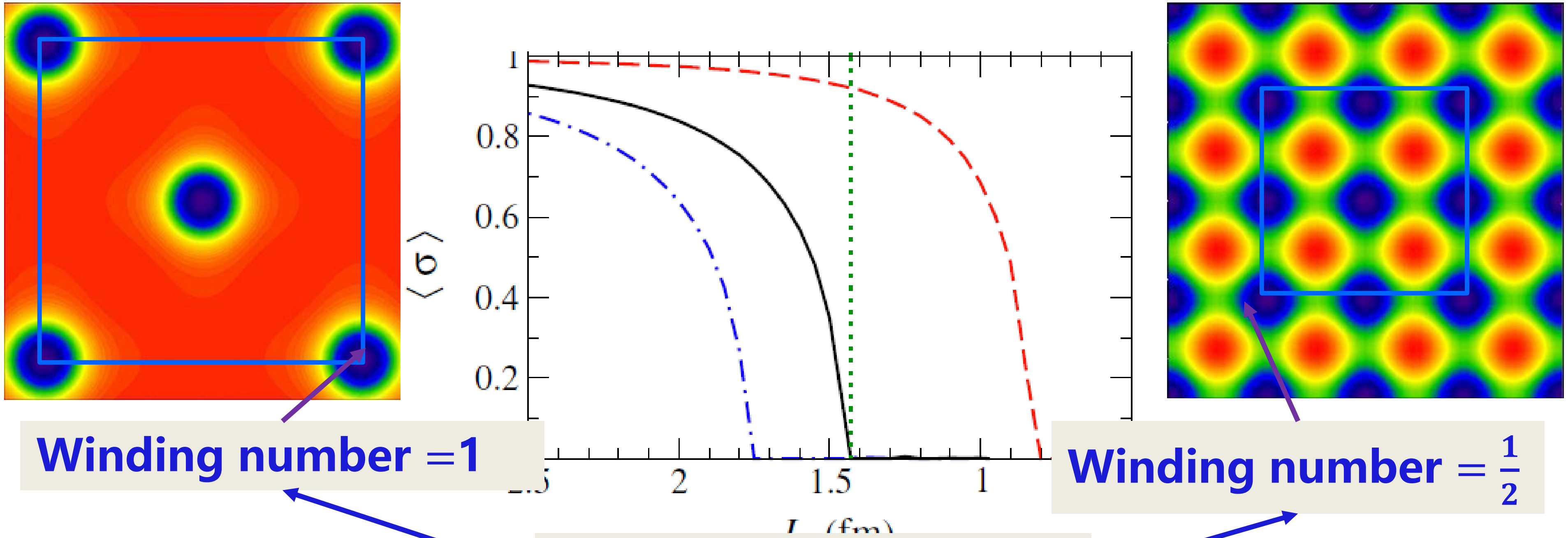

Winding number =1

Winding number $= \frac{1}{2}$

Topology transition

The half-skyrmion phase, characterized by the quark condensate $\Sigma \equiv \langle\bar{q}q\rangle$ vanishing on average but locally nonzero with chiral density wave and non-zero pion decay constant.

No phase transition!

Topology change: Parity doublet structure

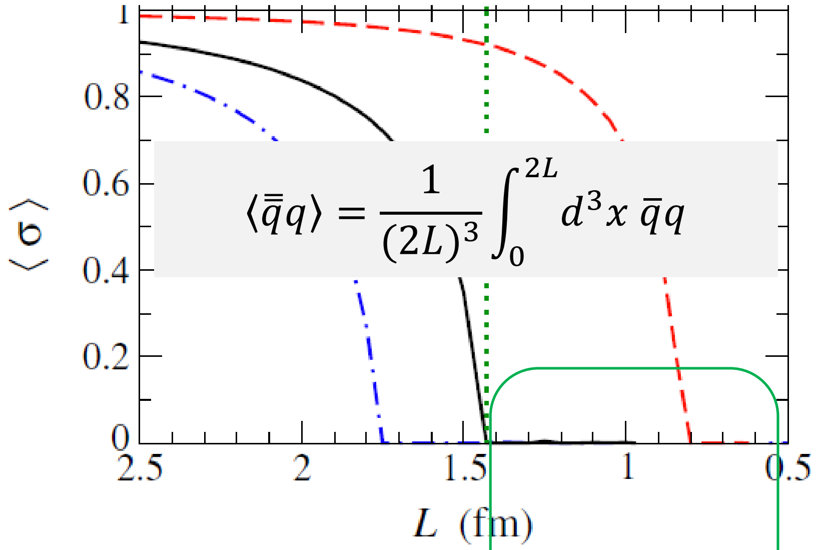

$$\langle \bar{q}q \rangle = \frac{1}{(2L)^3} \int_0^{2L} d^3x \, \bar{q}q$$

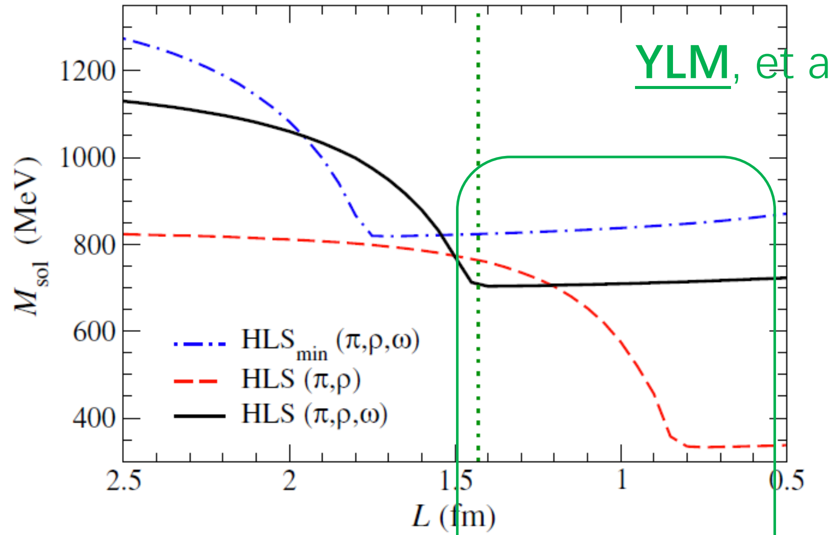

YLM, et al, PRD 13', 14'

High density region(small L): **Quark condensate vanishes** **However** **Nucleon mass is non-zero**

- **Nucleon mass is not solely from chiral symmetry breaking, it include a chiral invariant part. parity doubling structure.**

Agree with Y. Motohiro, *et al*, Phys.Rev. C92 (2015), 025201

Topology change and quark-hadron continuity

$$E(n,\alpha) = E(n,\alpha=0) + E_{\rm sym}(n)\alpha^2 + O(\alpha^4) + \cdots$$

"Symmetry energy is dominated by the tensor forces":

$$E_{sym} \propto 1/\lambda_I + O(1/N_c^2).$$

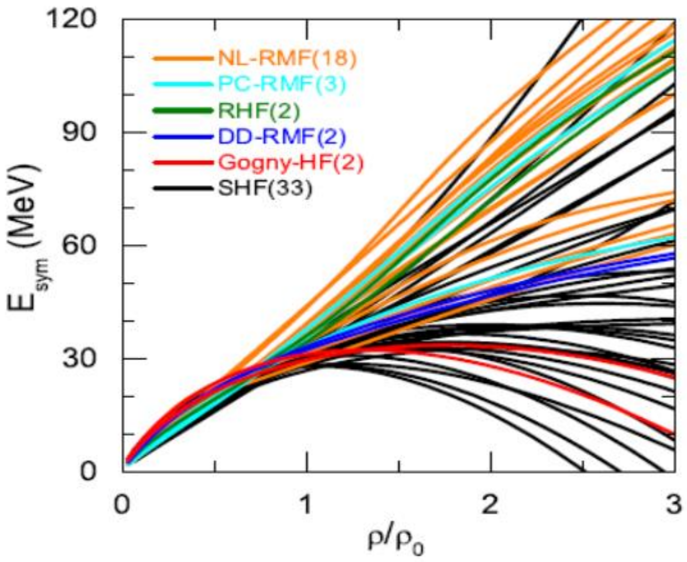

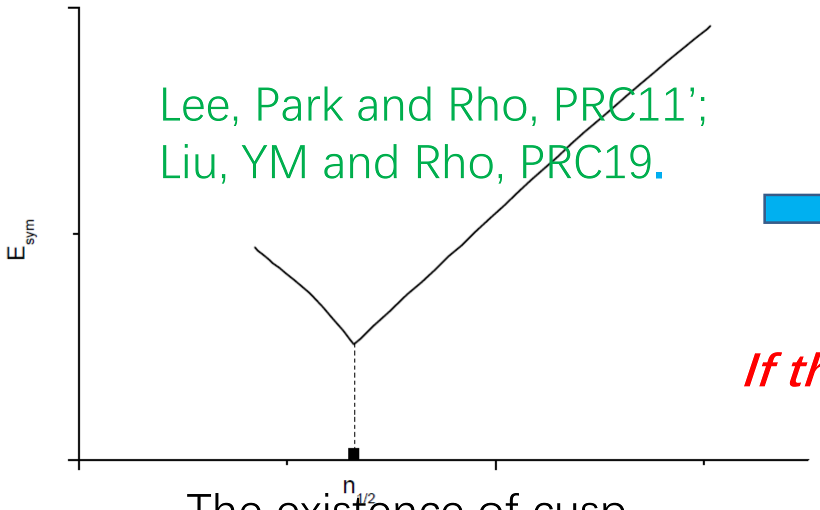

The existence of cusp
is model independent.

With nuclear correlations

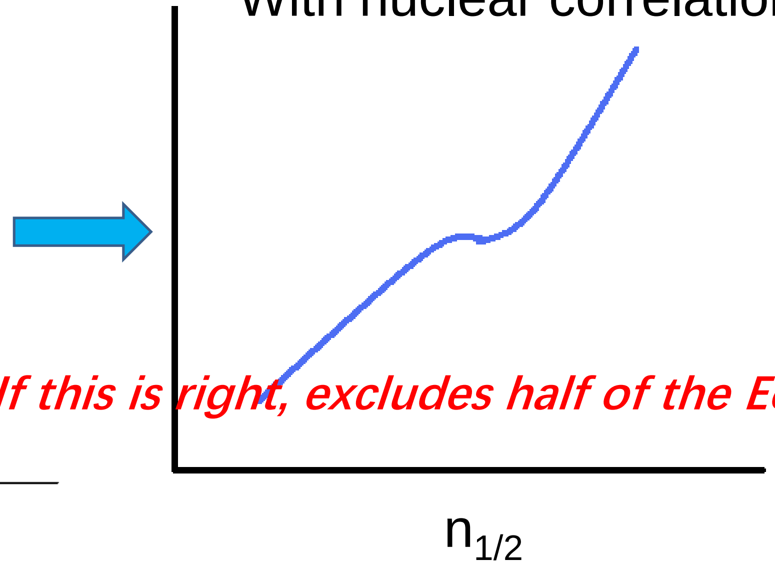

If this is right, excludes half of the EoS !

The cusp is associated with the topology change with the emergence of quasiparticle structure with the half-skyrmions.

Topology change and quark-hadron continuity

G.E. Brown and R. Machleidt 1994 … A. (

$$E_{sym} \approx c\,\frac{\langle (V^T)^2\rangle}{\Delta E}$$

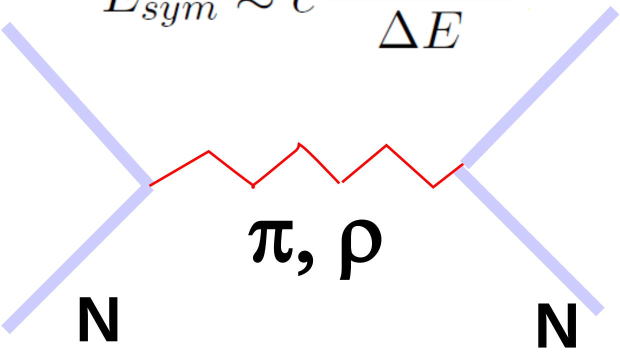

$$V_M^T(r) = S_M \frac{f_{NM}^2}{4\pi} m_M \tau_1 \cdot \tau_2 S_{12} \left(\left[\frac{1}{(m_M r)^3} + \frac{1}{(m_M r)^2} + \frac{1}{3 m_M r} \right] e^{-m_M r} \right)$$

$$M = \pi, \rho,\ S_{\rho(\pi)} = +1(-1)$$

$$R_M^* \equiv \frac{f_{NM}^*}{f_{NM}} \approx \frac{g_{MNN}^*}{g_{MNN}} \frac{m_N}{m_N^*} \frac{m_M^*}{m_M}$$

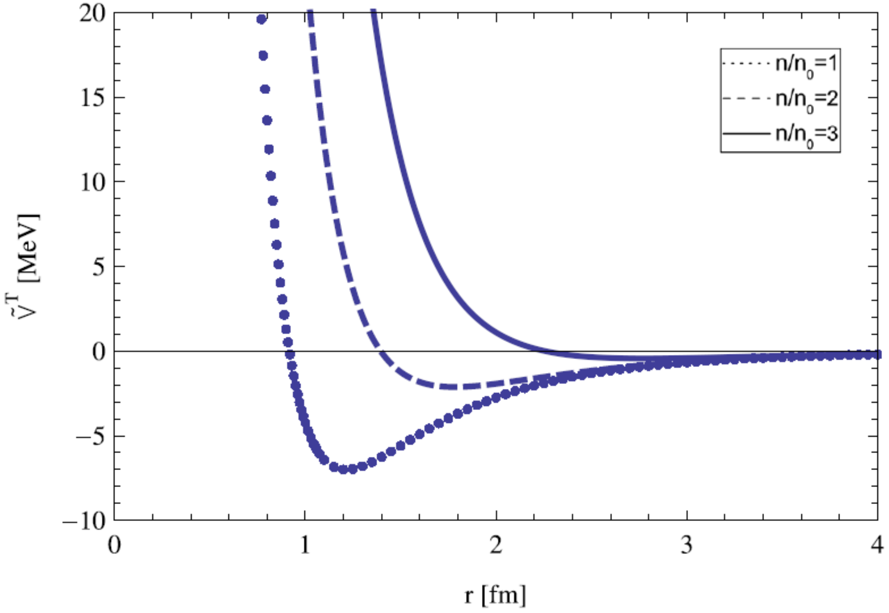

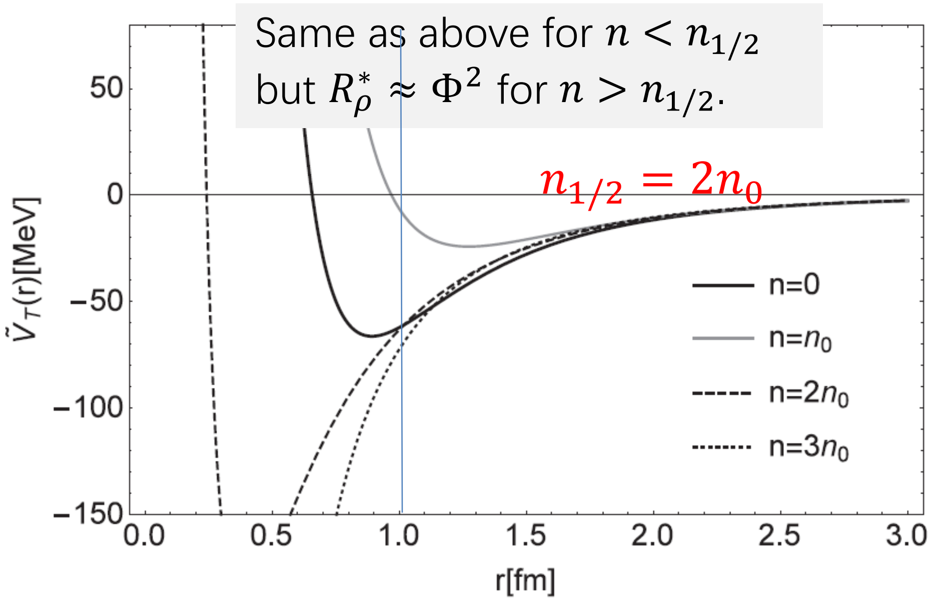

The Cheshire Cat

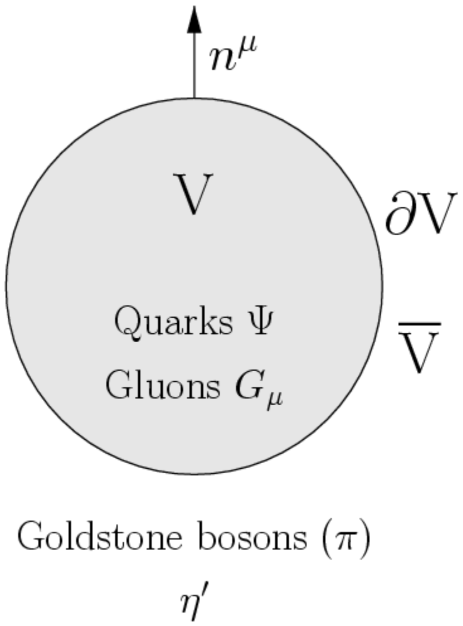

"How hadrons transform to quarks"

Baryon charge:

$$B_{out} = \frac{1}{\pi}[\theta(R) - \frac{1}{2}\sin 2\theta(R)]$$

$$B_{in} = 1 - \frac{1}{\pi}[\theta(R) - \frac{1}{2}\sin 2\theta(R)]$$

$$B = B_{out} + B_{in} = 1$$

Brown, Goldhaber, Rho 1983
Goldstone, Jaffe 1983

Topology change and quark-hadron continuity

Proton

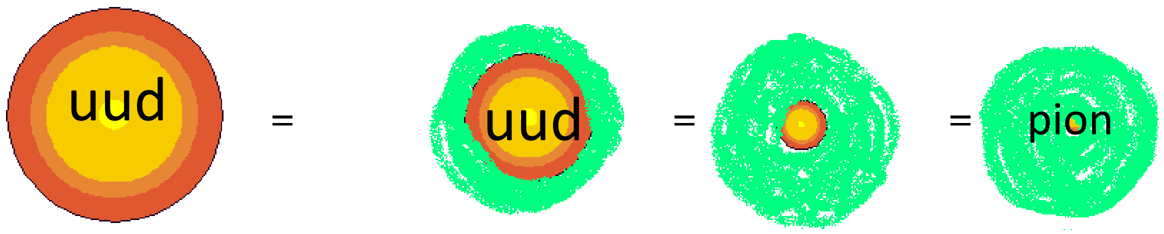

Equivalent description of the proton

$$S = S_V + S_{\overline{V}} + S_{\delta V},$$

where

$$S_V = \int_V d^4x \left(\bar{\psi} i \not{D} \psi - \frac{1}{2}\mathrm{tr}\, G_{\mu\nu}G^{\mu\nu}\right) + \cdots,$$

$$S_{\overline{V}} = \frac{f^2}{4}\int_{\overline{V}} d^4x \left(\mathrm{Tr}\, \partial_\mu U^\dagger \partial^\mu U + \frac{1}{4N_f} m_{\eta'}^2 (\mathrm{Tr}\ln U - \mathrm{Tr}\ln U^\dagger)^2\right) + S_{WZ} + \cdots,$$

$$S_{\delta V} = \frac{1}{2}\int_{\delta V} d\Sigma^\mu \left\{ (n_\mu \bar{\psi} U^{\gamma_5} \psi) + i\frac{g_s^2}{16\pi^2} K_{5\mu} (\mathrm{Tr}\ \ln U^\dagger - \mathrm{Tr}\ \ln U) \right\}.$$

$$K_5^\mu = \epsilon^{\mu\nu\alpha\beta}(G_\nu^a G_{\alpha\beta}^a - \frac{2}{3} g_s f^{abc} G_\nu^a G_\alpha^b G_\beta^c),$$

Flavor singlet axial charge gA(0) (Lee et al)

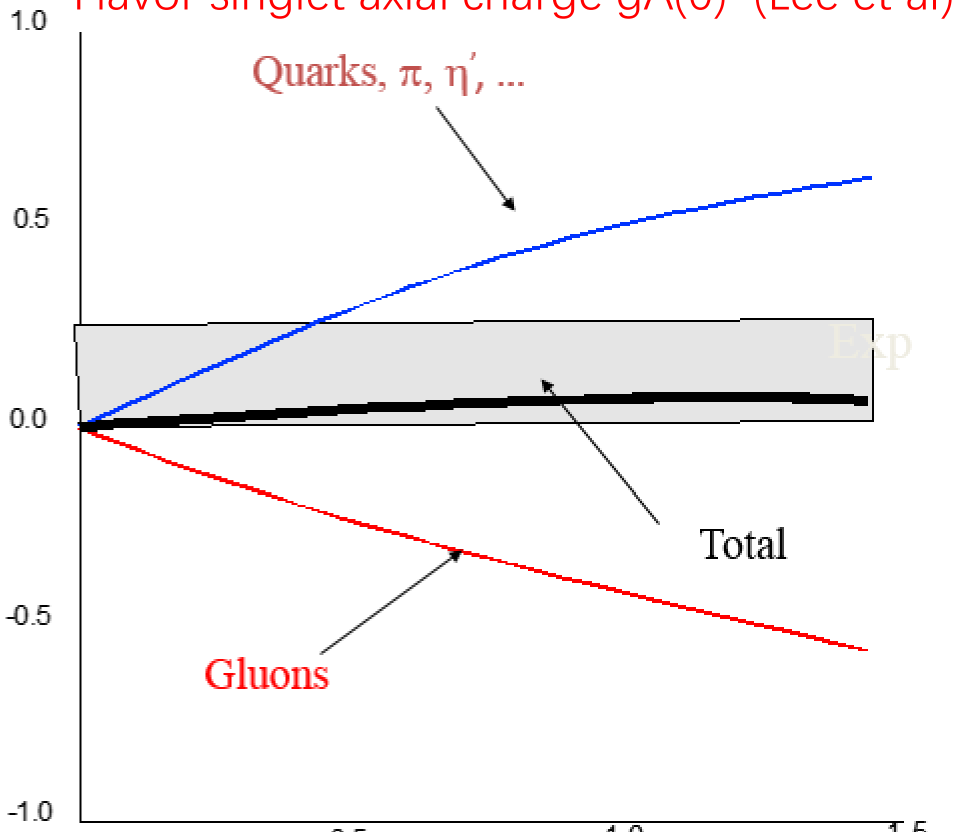

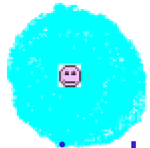

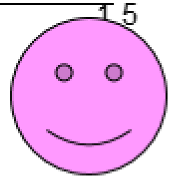

When the bag radius is shrunk to zero, only the smile of the cat is left with spinning gapless quarks running luminally

Topology change and quark-hadron continuity

When $N_f = 1$,

Since $\pi_3(U(1)) = 0$;

Rule out the skyrmion approach?

$$J_{\alpha\beta\gamma} = \epsilon_{\alpha\beta\gamma\delta}\partial^{\delta}\eta'/2\pi$$

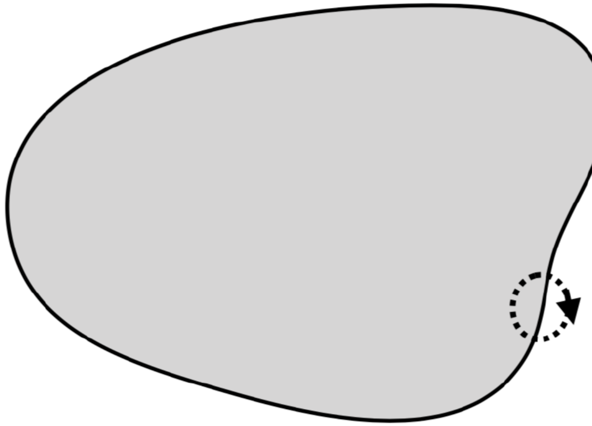

Baryons as Quantum Hall Droplets

ep-th] 6 Feb 2019

1812.09253 [hep-th]

Zohar Komargodski

Simons Center for Geometry and Physics, Stony Brook, New York, USA
and Weizmann Institute of Science, Rehovot 76100, Israel

Abstract

$N_f = 1$ baryon can be interpreted as quantum Hall droplet. An important element in the construction is an extended, $2+1$dimensional, meta-stable configuration of the η' particle. Baryon number is identified with a magnetic symmetry on the $2+1$ sheet.

are able to determine the spin, isospin, and certain excitations of the droplet. In addition, balancing the tension of the droplet against the energy stored at the boundary we estimate the size and mass of the baryons. The mass, size, spin, isospin, and excitations that we find agree with phenomenological expectations.

Topology change and quark-hadron continuity

YLM, Nowak, Rho & Zahed, 1907.00958

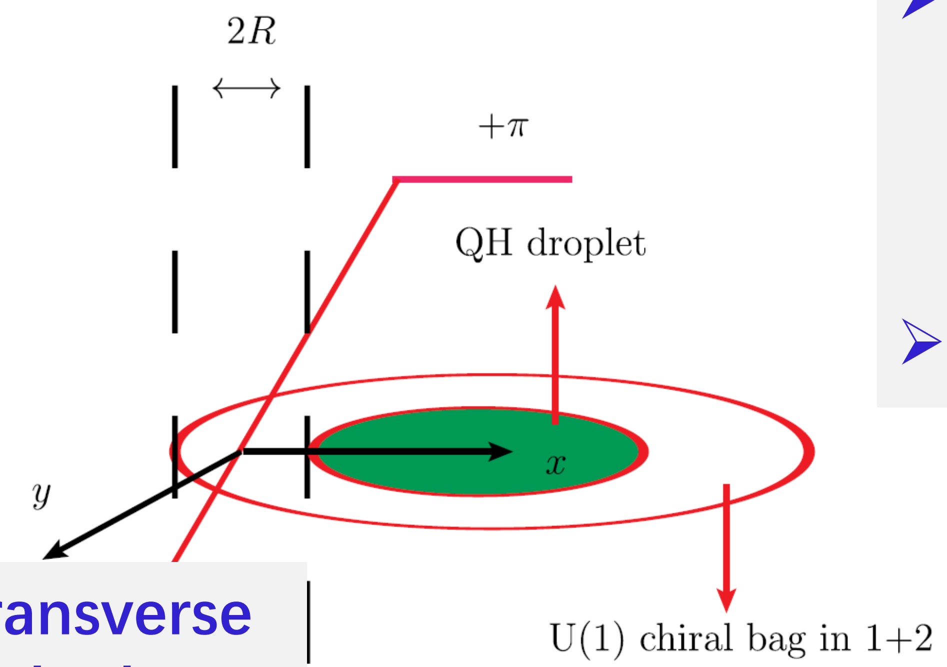

- Consists of free 2-dim quarks, charge e, and subject to a chiral bag BC along the radial x-direction.
- Leaks most quantum numbers.

A current transverse to the smile is shown to appear.
Hall current.

- Annulus of radius R and clouded by an η'-field with a monodromy of 2π.
- The bag radius is immaterial thanks to CCP.

Topology change and quark-hadron continuity

国科大杭州高等研究院 Hangzhou Institute For Advanced Study,UCAS

PHYSICAL REVIEW LETTERS **123,** 172301 (2019)

Baryon as a Quantum Hall Droplet and the Quark-Hadron Duality

Yong-Liang Ma,[1,*] Maciej A. Nowak,[2,†] Mannque Rho,[3,‡] and Ismail Zahed[4,§]

[1]*Center for Theoretical Physics and College of Physics, Jilin University, Changchun 130012, China*

[2]*Marian Smoluchowski Institute of Physics and Mark Kac Complex Systems Research Center, Jagiellonian University, ulica Stanisł awa Łojasiewicza 11, PL 30-348 Kraków, Poland*

[3]*Institut de Physique Theorique, CEA Saclay, 91191 Gif-sur-Yvette cedex, France*

[4]*Department of Physics and Astronomy, Stony Brook University, Stony Brook, New York 11794–3800, USA*

(Received 12 July 2019; revised manuscript received 2 September 2019; published 22 October 2019)

- 利用重子的手征口袋模型阐明了致密核物质中的夸克-强子对偶机制；
- 给出了在强子物理中实现凝聚态物理中的一些概念的范例。

topological field theory due to the Callan-Harvey anomaly outflow. The chiral bag naturally carries the unit baryon number and spin $\frac{1}{2}N_c$. The generalization to arbitrary N_f is discussed.

DOI: 10.1103/PhysRevLett.123.172301

Hidden symmetries of QCD

Rho and omega mesons play an important role in our formalism of compact star structure

Redundancy in the decomposition

$$U(x) = \xi_L \; h(x)\, h(x)^\dagger \; \xi_R{}^\dagger$$

$$h(x) \in SU(2)_{L+R} \times U(1)_{L+R}$$

ρ meson

ω meson

The idea -- that is totally different from what one could call "standard" in nuclear community - is that ρ (and ω, in a different way) is "hidden gauge field".

Bando, *et al* 89; Harada & Yamawaki, 03

$$\hat{\alpha}_{\parallel\mu} = \frac{1}{2i}(D_\mu \xi_R \cdot \xi_R^\dagger + D_\mu \xi_L \cdot \xi_L^\dagger),$$

$$\hat{\alpha}_{\perp\mu} = \frac{1}{2i}(D_\mu \xi_R \cdot \xi_R^\dagger - D_\mu \xi_L \cdot \xi_L^\dagger) \,,$$

$$V_\mu(x) = \frac{g_\rho}{2}\rho_\mu^a \tau^a + \frac{g_\omega}{2}\omega_\mu I_{2\times 2},$$

$$\mathcal{L}_M = f_\pi^2 \mathrm{tr}\left[\hat{\alpha}_{\perp\mu}\hat{\alpha}_\perp^\mu\right] + a_\rho f_\pi^2 \mathrm{tr}\left[\hat{\alpha}_{\parallel\mu}\hat{\alpha}_\parallel^\mu\right] + (a_\omega - a_\rho) f_\pi^2 \mathrm{tr}\left[\hat{\alpha}_{\parallel\mu}\right] \mathrm{tr}\left[\hat{\alpha}_\parallel^\mu\right] - \frac{1}{2}\mathrm{tr}\left[\rho_{\mu\nu}\rho^{\mu\nu}\right] - \frac{1}{2}\mathrm{tr}\left[\omega_{\mu\nu}\omega^{\mu\nu}\right] .$$

It captures extremely well certain strong interaction dynamics even at tree order.

Hidden symmetries of QCD

$f_0(500)$ is a pNGB arising from (noted $m_{f_0} \cong m_K$). The SB of SS associated + an explicit breaking of SI.

Assumption: There is an Nonperturbative IR fixed point in the running QCD coupling constant α_s.

EB of SI: Departure of α_s from IRFP + current quark mass.

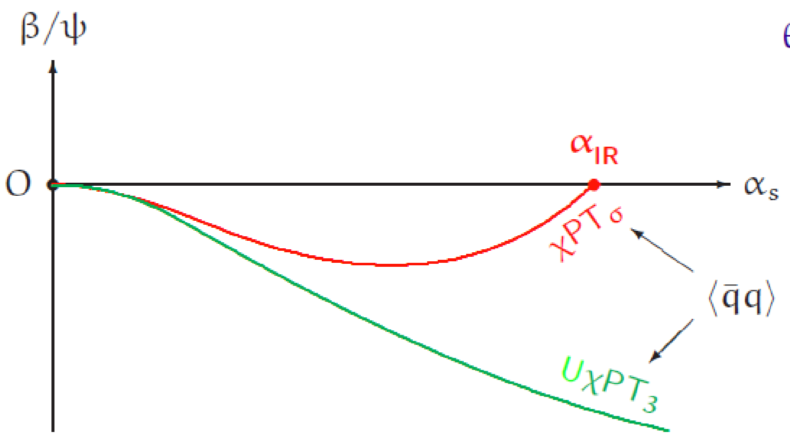

$$\theta^\mu_\mu = \frac{\beta(\alpha_s)}{4\alpha_s} G^2 + (1+\gamma_m) \sum_{q=u,d,s} m_q \bar{q} q$$

IR fixed point: $\beta(\alpha_{IR}) = 0$

$\chi PT_\sigma \Rightarrow$ expand in θ^μ_μ

$\alpha_s \lesssim \alpha_{IR}$, $m_{u,d,s} \sim 0$

about scale-*dependent* $|vac\rangle$

$\Rightarrow$ NG bosons π, K, η, σ.

$$\mathcal{L}^{LO}_{\chi PT_\sigma} = \mathcal{L}^{d=4}_{inv} + \mathcal{L}^{d>4}_{anom} + \mathcal{L}^{d<4}_{mass},$$

$$\mathcal{L}^{d=4}_{inv} = c_1 \frac{f_\pi^2}{4}\left(\frac{\chi}{f_\chi}\right)^2 \mathrm{Tr}\left(\partial_\mu U \partial^\mu U^\dagger\right) + \frac{1}{2} c_2 \partial_\mu \chi \partial^\mu \chi + c_3 \left(\frac{\chi}{f_\chi}\right)^4,$$

$$\mathcal{L}^{d>4}_{anom} = (1-c_1)\frac{f_\pi^2}{4}\left(\frac{\chi}{f_\chi}\right)^{2+\beta'} \mathrm{Tr}\left(\partial_\mu U \partial^\mu U^\dagger\right) + \frac{1}{2}(1-c_2)\left(\frac{\chi}{f_\chi}\right)^{\beta'} \partial_\mu \chi \partial^\mu \chi + c_4 \left(\frac{\chi}{f_\chi}\right)^{4+\beta'},$$

$$\mathcal{L}^{d<4}_{mass} = \frac{f_\pi^2}{4}\left(\frac{\chi}{f_\chi}\right)^{3-\gamma_m} \mathrm{Tr}\left(\mathcal{M}^\dagger U + U^\dagger \mathcal{M}\right),$$

Crewther and Tunstall , PR**D91**, 034016

Provides an approach to include scalar meson in ChPT.

Hidden symmetries of QCD

$$\mathcal{L}_N = \bar{Q} i\gamma^\mu D_\mu Q - g_1 F_\pi \frac{\chi}{F_\chi} \bar{Q}Q + g_2 F_\pi \frac{\chi}{F_\chi} \bar{Q}\rho_3 Q$$
$$- i m_0 \bar{Q}\rho_2\gamma_5 Q + g_{V\rho}\bar{Q}\gamma^\mu \hat{\alpha}_{\parallel\mu} Q$$
$$+ g_{V0}\bar{Q}\gamma^\mu \mathrm{tr}[\hat{\alpha}_{\parallel\mu}]Q + g_A \bar{Q}\rho_3\gamma^\mu \hat{\alpha}_{\perp\mu}\gamma_5 Q,$$

- Beane and Klock, PLB, 94'
- Paeng, Lee, Rho and Sasaki, 12'

$$\Sigma = U\chi \frac{F_\pi}{F_\chi} = s + i\vec{\tau}\cdot\vec{\pi}$$

$$m_{N_\pm} = \mp g_2\langle s\rangle + \sqrt{(g_1\langle s\rangle)^2 + m_0^2},$$

$\langle s\rangle \to 0$

$$g_{v\rho} - g_A \to 0, \quad \alpha - 1 \to 0. \quad \alpha \equiv f_\pi^2/f_\chi^2$$

$$m_{N_\pm} \to m_0.$$

Chiral inv. mass

$$\mathcal{L}_N = \bar{N}i\partial\!\!\!/ N - \bar{N}\hat{M}N - g_1\bar{N}\left(\hat{G}\tilde{s} + \rho_3\gamma_5 i\vec{\tau}\cdot\vec{\tilde{\pi}}\right)N$$
$$+ g_2\bar{N}\left(\rho_3\tilde{s} + \hat{G}\gamma_5 i\vec{\tau}\cdot\vec{\tilde{\pi}}\right)N$$
$$+ (1 - g_{v\omega})\, g_\omega N\frac{\omega\!\!\!/}{2}N\,,$$

$$g_{\rho NN} = g_\rho(g_{v\rho} - 1) \to 0.$$

ρ decouples, HFS emerges.

Proposition: *Moving toward to the dilaton-limit fixed point, the fundamental constants in scale-chiral symmetry get transformed as $f_\pi \to f_\chi$, $g_A \to g_{v\rho} \to 1$, and the ρ meson decouples while the ω remains coupled, breaking the flavor $U(2)$ symmetry.*

Hidden symmetries of QCD

Emergent from parameter dialing from RMF:

$$\mathcal{L} = \bar{N} i\gamma^\mu D_\mu N - h f_\pi \frac{\chi}{f_\chi}\bar{N}N + g_{v\rho}\bar{N}\gamma^\mu \hat{\alpha}_{\parallel\mu} N + g_{v0}\bar{N}\gamma^\mu \mathrm{Tr}\left[\hat{\alpha}_{\parallel\mu}\right] \mathrm{N} + \mathrm{g_A}\bar{\mathrm{N}}\gamma^\mu \hat{\alpha}_{\perp\mu}\gamma_5 \mathrm{N} + \mathrm{V}(\chi)$$

Paeng, Lee, Rho and Sasaki, PRD 13'.

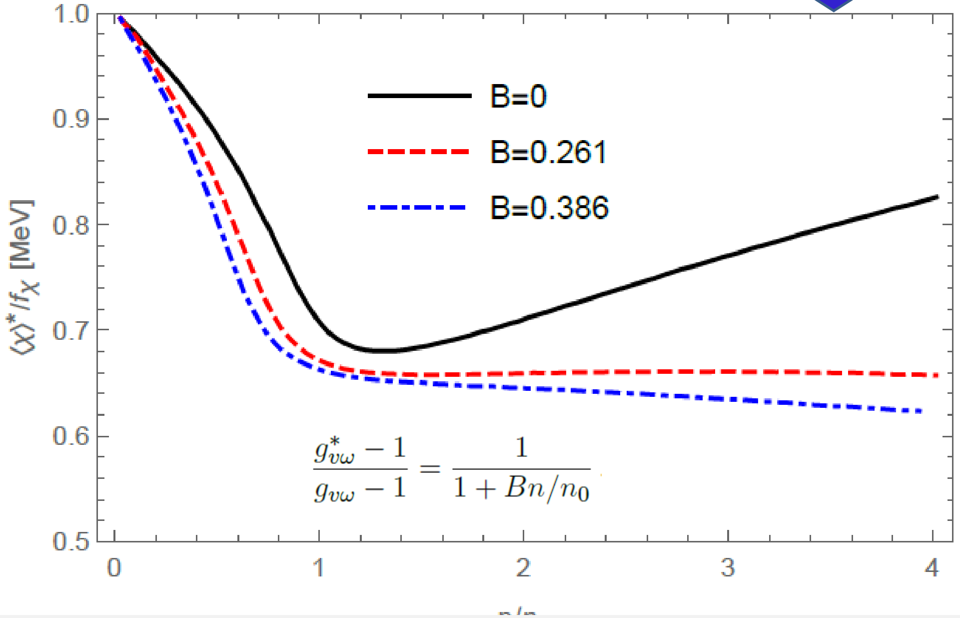

Parity doubling emerges via an interplay between ω–N *coupling -- with* $U(2)$ *symmetry strongly broken -- and the dilaton condensate.*

$$\langle\theta^\mu_\mu\rangle = \langle\theta^{00}\rangle - \sum_i \langle\theta^{ii}\rangle = \epsilon - 3P$$

$$= 4V(\langle\chi\rangle) - \langle\chi\rangle \left.\frac{\partial V(\chi)}{\partial\chi}\right|_{\chi=\langle\chi\rangle}$$

In the MF of bsHLS, the TEMT is given solely by the dilaton condensate.

Proposition: *Going toward the DLFP with the ρ decoupling from the nucleons, the parity doubling emerges and* $m_N^* \to \langle\chi\rangle^* \to m_0$.

$$\mathcal{L} = \mathcal{L}^{M}_{\chi PT_\sigma}(\pi, \chi, V_\mu) + \mathcal{L}^{B}_{\chi PT_\sigma}(\psi, \pi, \chi, V_\mu) - V(\chi)$$

$$\mathcal{L}^{M}_{\chi PT_\sigma}(\pi, \chi, V_\mu) = f_\pi^2 \left(\frac{\chi}{f_\sigma}\right)^2 \mathrm{Tr}[\hat{a}_{\perp\mu}\hat{a}^{\mu}_{\perp}] + a f_\pi^2 \left(\frac{\chi}{f_\sigma}\right)^2 \mathrm{Tr}[\hat{a}_{\parallel\mu}\hat{a}^{\mu}_{\parallel}] + \frac{1}{2g^2}\mathrm{Tr}[V_{\mu\nu}V^{\mu\nu}] + \frac{1}{2}\partial_\mu\chi\partial^\mu\chi$$

$$\mathcal{L}^{B}_{\chi PT_\sigma}(\psi, \pi, \chi, V_\mu) = \mathrm{Tr}(\bar{B} i\gamma_\mu D^\mu B) - \frac{\chi}{f_\sigma}\mathrm{Tr}(\bar{B}B) + \cdots$$

$$V(\chi) \approx \frac{m_\sigma^2 f_\sigma^2}{4}\left(\frac{\chi}{f_\sigma}\right)^4 \left[\ln\left(\frac{\chi}{f_\sigma}\right) - \frac{1}{4}\right].$$

Only in terms of hadrons;

Intrinsic density dependence;

EFT matching.

- Enters through the VeV of dilaton: scale symmetry;
- Information from topology change is considered;
- Nucleon mass stays as a constant after topology change: parity doublet.
- *The topology change density $n_{1/2}$, parameter.*

Cashire Cat

Quark-Hadron continuity

Qualitative information from topology change

Density dependence of LECs

Topology change and quark-hadron continuity

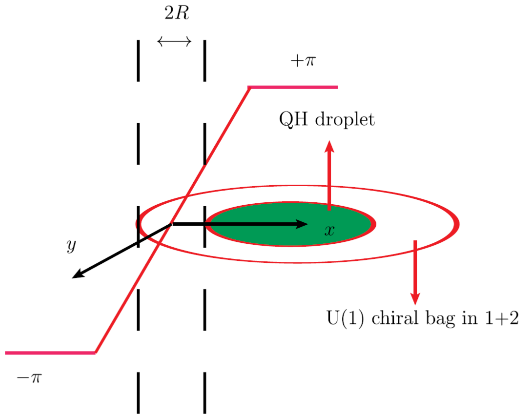

PHYSICAL REVIEW LETTERS **123,** 172301 (2019)

Baryon as a Quantum Hall Droplet and the Quark-Hadron Duality

Yong-Liang Ma,[1,*] Maciej A. Nowak,[2,†] Mannque Rho,[3,‡] and Ismail Zahed[4,§]
enter for Theoretical Physics and College of Physics, Jilin University, Changchun 130012, China
oluchowski Institute of Physics and Mark Kac Complex Systems Research Center, Jagiellonian University, ulica Stanisł awa Łojasiewicza 11, PL 30-348 Kraków, Poland
[3]*Institut de Physique Theorique, CEA Saclay, 91191 Gif-sur-Yvette cedex, France*
[4]*Department of Physics and Astronomy, Stony Brook University, Stony Brook, New York 11794–3800, USA*

(Received 12 July 2019; revised manuscript received 2 September 2019; published 22 October 2019)

- 利用重子的手征口袋模型阐明了致密核物质中的夸克-强子对偶机制；
- 给出了在强子物理中实现凝聚态物理中的一些概念的范例。

topological field theory due to the Callan-Harvey anomaly outflow. The chiral bag naturally carries the unit baryon number and spin $\frac{1}{2}N_c$. The generalization to arbitrary N_f is discussed.

DOI: 10.1103/PhysRevLett.123.172301

$$g_A^{eff} = g_A^{free} \times q$$

For $A \leq 60$ nuclei

In shell model

$$g_A^{eff} = q_{light} \times g_A^{free} \approx 0.98 - 1.18$$

Pick typical value

$$q_{light} \approx 0.78$$

For $A > 60$ nuclei

C.B. Henke, et al., Nature, 2012'

Old GSI: $B_{GT}^{GSI} = 9.1_{-3.0}^{+2.6}$

ESPM: $B_{GT}^{ESPM} = 17.78$

$q_{GSI}^{ESPM} = 0.6 - 0.8$

T. Faestermann, et al, PPNP 13'

Recent RIKEN: $B_{GT}^{RIKEN} = 4.4_{-0.7}^{+0.9}$

D. Lubos, et al., PRL 19'

$$q_{RIKEN}^{ESPM} = 0.46 - 0.55$$

Offers a glimpse into how scale symmetry manifests in dense baryonic matter.

$$q_{G\sigma EFT}^{ESPM} = q_{SSB} \times q_{SNC}$$

In ***GσEFT***, axial current

$$q_{SSB} g_A \overline{\psi} \tau^{\pm} \gamma_\mu \gamma_5 \psi$$

$$q_{SSB} = c_A + (1 - c_A)\Phi^{\beta'}$$

- In the vacuum, $\Phi = 1$, so the β' dependence is absent. In nature the scalar mass is nonzero, so $\beta' \neq 0$.
- In the medium

$$\Phi(n) = \frac{f_\chi^*(n)}{f_\chi} \simeq \frac{f_\pi^*(n)}{f_\pi} < 1 \text{ for } n \neq 0,$$

- f_π^* is known up to nuclear matter density by experiment.
- It is notable that the property of scale symmetry breaking in the GT operator appears entirely in the factor q_{SSB}.
- The β' representing scale anomaly, an explicit breaking, can figure with density dependence only when $c_A < 1$.

- Using FLFP with $\Phi(n_0) = 0.8$, $q_{SNC}^{Landau} \approx 0.79$. Thus in the LOSS

$$g_A^{Landau} \approx 1.0.$$

Very weakly dependent on density, good for both light and heavy nuclei.

Thus result, identified as the effect of nuclear correlations obtained in the LOSS without explicit β' dependence, **does not imply that $\boldsymbol{\beta'}$ is negligible.**

- To have an idea how things go,let's assume $c_A \approx 0.15$ and $\beta' \approx 2.0$ ---the same values that resolve the hWZ problem

$$q_{\mathrm{SSB}} = c_A + (1 - c_A)\Phi^{\beta'} \approx 0.63$$

⬇

$$q_{\mathrm{G\sigma EFT}}^{\mathrm{ESPM}} = q_{\mathrm{SSB}} \times q_{\mathrm{SNC}}^{\mathrm{Landau}} \approx 0.63 \times 0.79 \approx 0.50.$$

This could explain the RIKEN result if the RIKEN data turns out to be correct.

Patterns of scale symmetry from nuclei to dense matter

PHYSICAL REVIEW LETTERS **125**, 142501 (2020)

Quenched g_A in Nuclei and Emergent Scale Symmetry in Baryonic Matter

Yong-Liang Ma[1,2,3,*] and Mannque Rho[4,†]
[1] *School of Fundamental Physics and Mathematical Sciences, Hangzhou Institute for Advanced Study, UCAS, Hangzhou 310024, China*
[2] *International Centre for Theoretical Physics Asia-Pacific (ICTP-AP) (Beijing/Hangzhou), UCAS, Beijing 100190, China*
[3] *Center for Theoretical Physics and College of Physics, Jilin University, Changchun, 130012, China*

$$q_{ssb} = c_A + (1 - c_A)\Phi^{\beta'} \approx 0.63$$

表明了标度对称性在核物质（从低密度到高密度）的实现方式。

The recent RIKEN experiment on the quenched g_A in the superallowed Gamow-Teller transition from

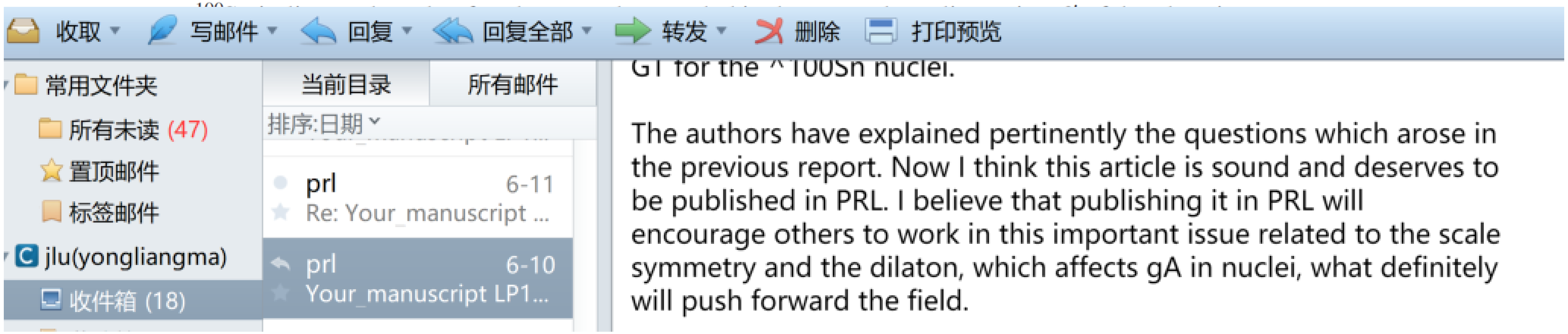

Implement topology transition to EoS

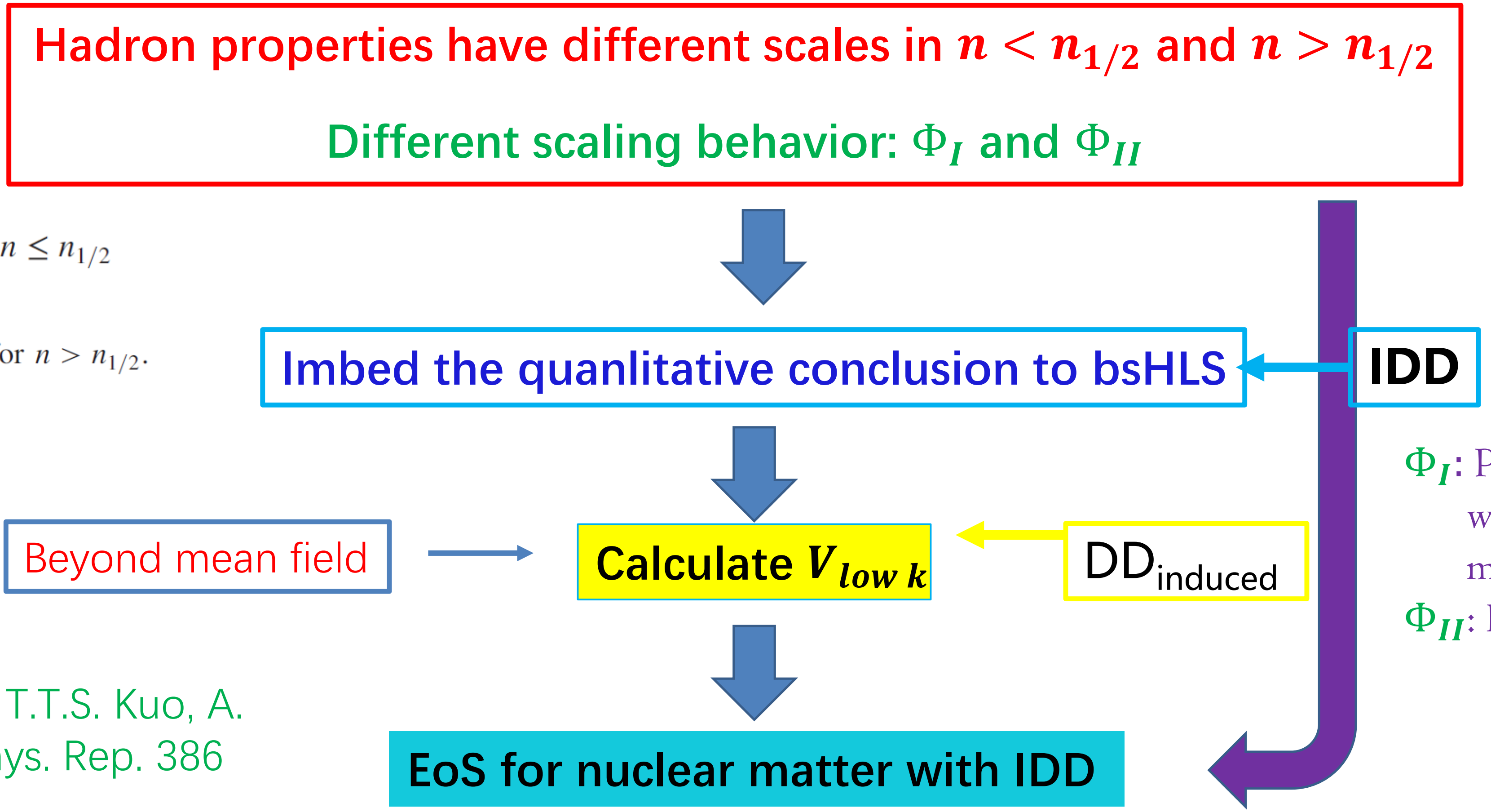

$$\Phi^* = \frac{1}{1 + c_I(n/n_0)} \quad \text{for } n \le n_{1/2}$$

$$\Phi^* \approx \kappa \approx \frac{1}{1 + c_I(n_{1/2}/n_0)} \quad \text{for } n > n_{1/2}.$$

$$g_\rho^*/g_\rho \approx 1 - n/n_{\rm VM}$$

Φ_I: Predictions agree with the nuclear matter at low density.

Φ_{II}: Density independent.

S.K. Bogner, T.T.S. Kuo, A. Schwenk, Phys. Rep. 386 (2003) .

Constraints around saturation density

TABLE III. Nuclear matter properties at $n_0 < n_{1/2}$. The empirical values are merely exemplary. n_0 is in unit fm^{-3} and others are in unit MeV.

Parameter	Prediction	Empirical
n_0	0.161	0.16 ± 0.01 [9]
B.E.	16.7	16.0 ± 1.0 [9]
$E_{sym}(n_0)$	30.2	31.7 ± 3.2 [10]
$E_{sym}(2n_0)$	56.4	46.9 ± 10.1 [11];40.2 ± 12.8 [12]
$L(n_0)$	67.8	58.9 ± 16 [11];58.7 ± 28.1 [10]
K_0	250.0	230 ± 20 [13]

Agrees with the empirical values of the nuclear matter properties quite well.

YLM & M. Rho, 2006.14173 v1

Equation of state

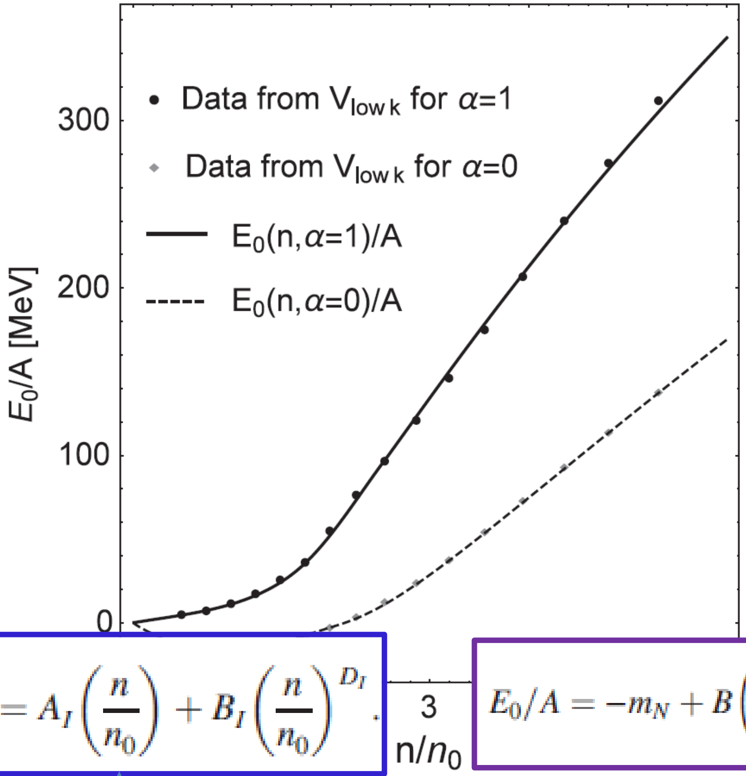

$$E_0/A = A_I\left(\frac{n}{n_0}\right) + B_I\left(\frac{n}{n_0}\right)^{D_I}$$

Fitted function

$$E_0/A = -m_N + B\left(\frac{n}{n_0}\right)^{1/3} + D\left(\frac{n}{n_0}\right)^{-1}$$

PC Prediction

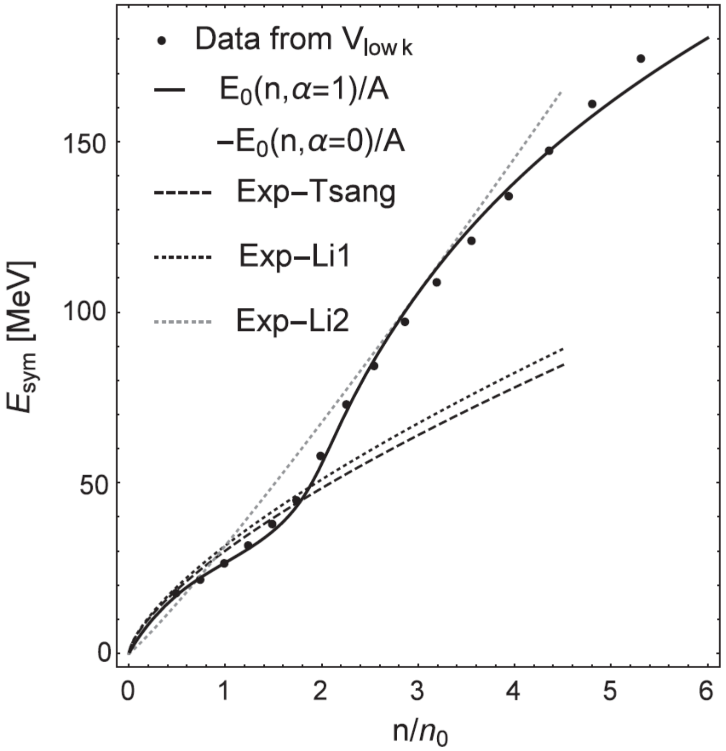

Equation of state

$$\frac{\partial}{\partial n}\langle\theta^{\mu}_{\mu}\rangle = \frac{\partial\epsilon(n)}{\partial n}(1-3v_s^2) = 0 \qquad v_s^2/c^2 = \frac{\partial P(n)}{\partial n}\Big/\frac{\partial\epsilon(n)}{\partial n}$$

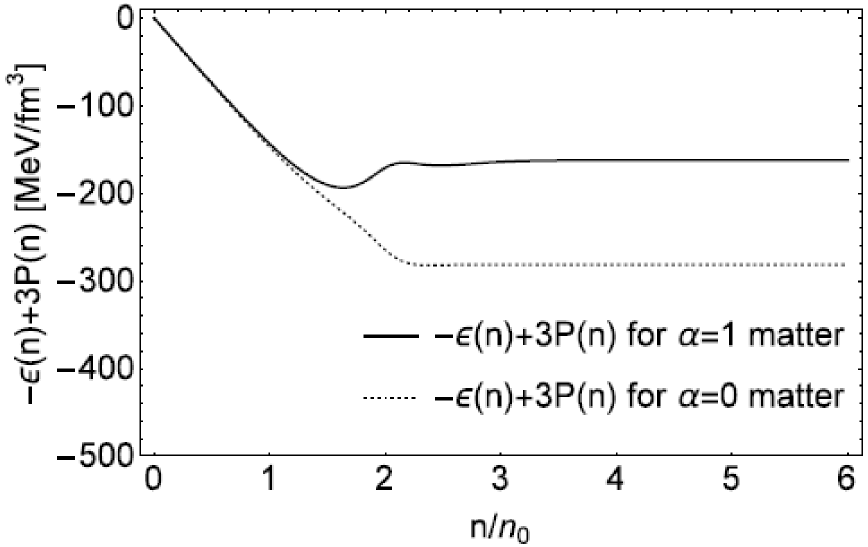

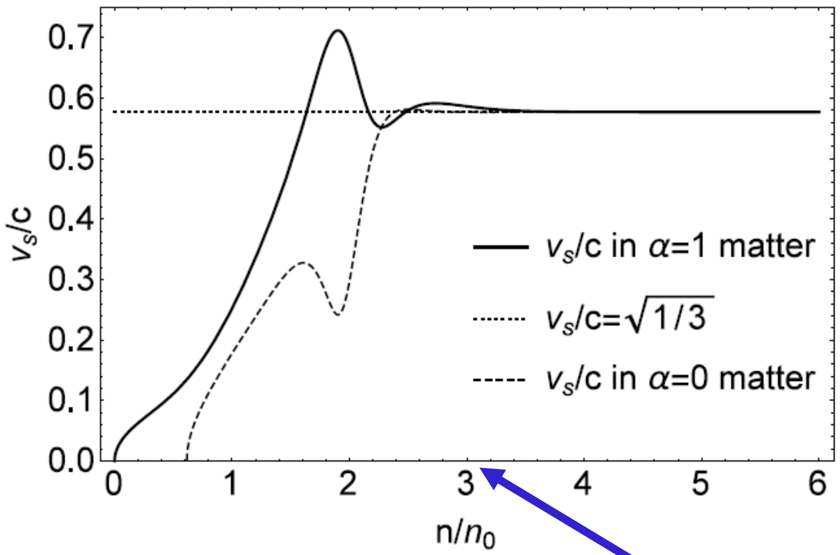

YLM et al, 1804.00305; 1811.07071

- Trace of energy-momentum tensor is not zero but a density independent constant at $\geq 2n_0$;
- When $\geq 2n_0$, the sound velocity $\rightarrow 1/\sqrt{3}$ -- conformal sound velocity.

Low density relevant to NSs

A feature NOT shared by ANY other models or theories in the field

国科大杭州高等研究院
Hangzhou Institute For Advanced Study,UCAS

Equation of state

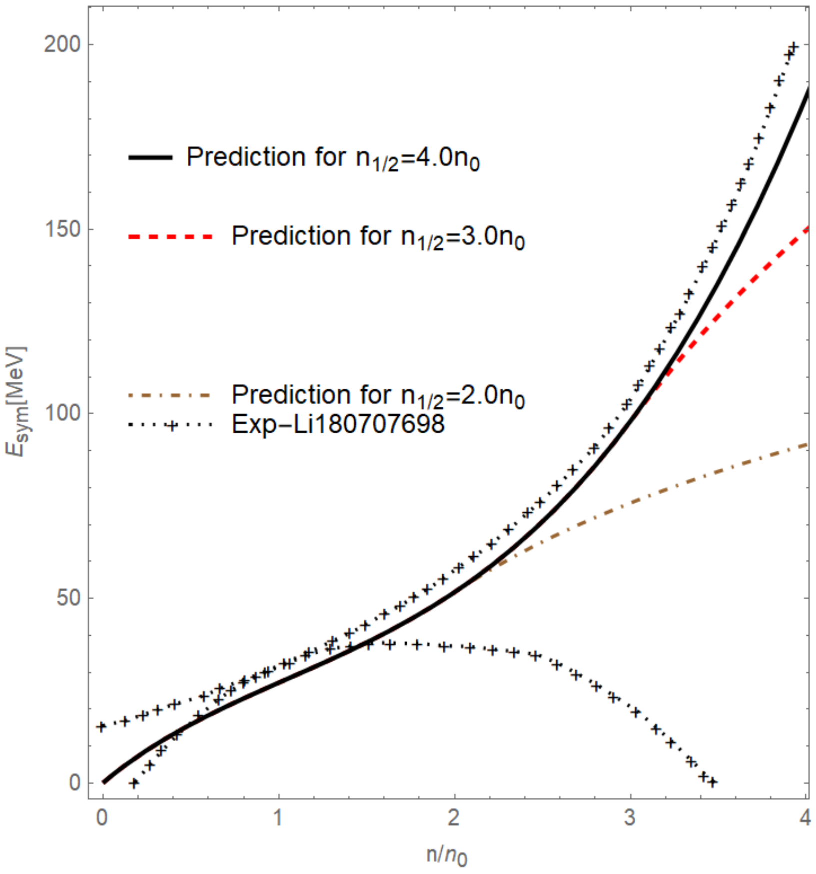

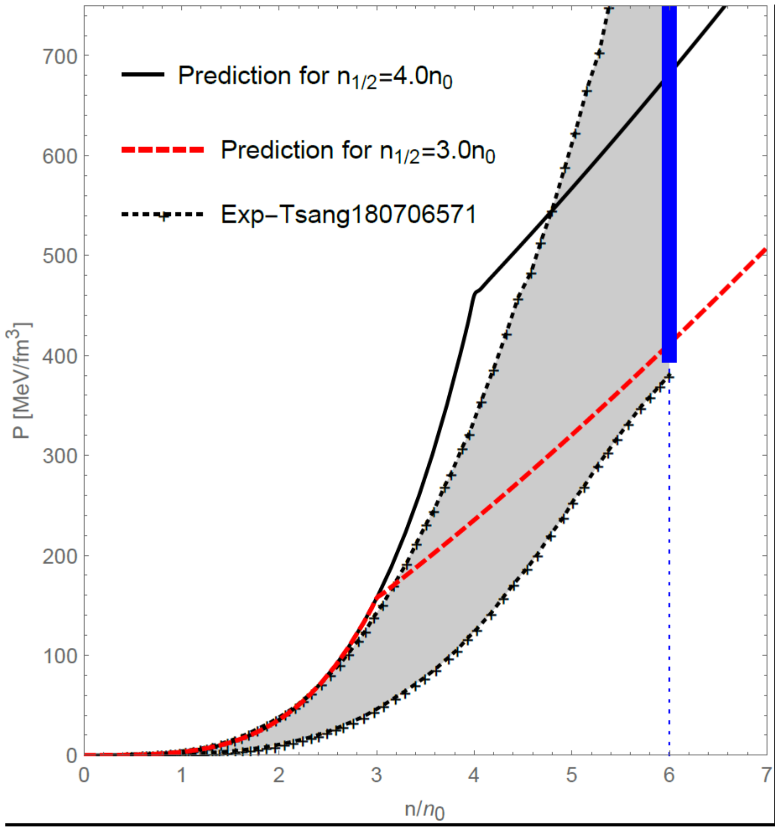

Agree with the constraints $n_{1/2}$ is constrained as $\sim(2\ -4\ )n_0$

Star properties

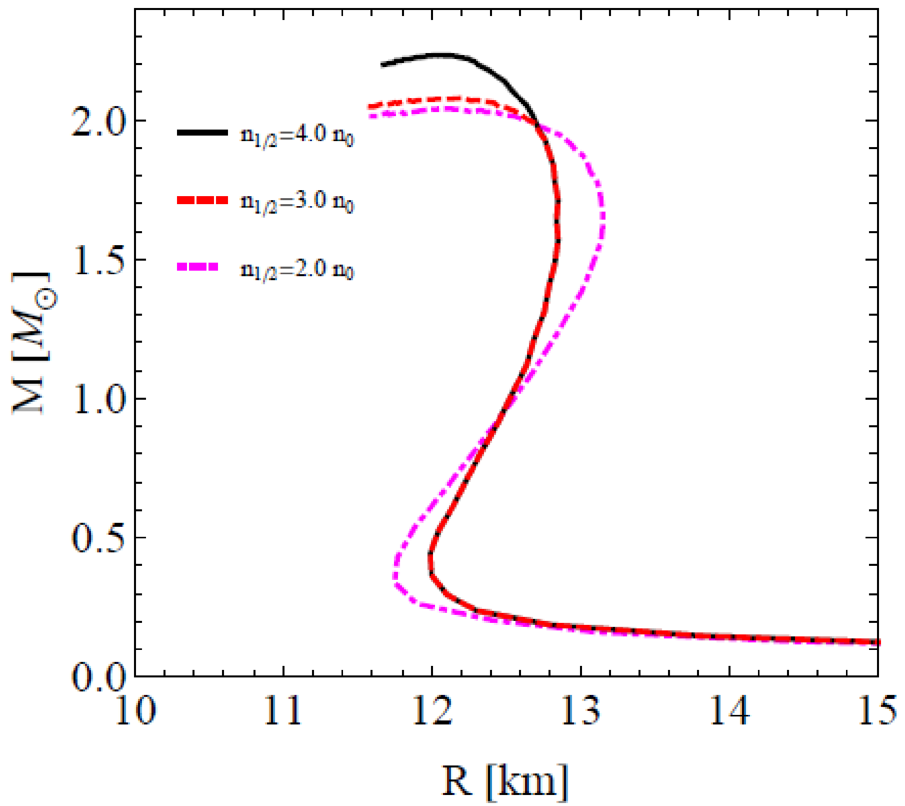

Accommodate massive star $\geq 2.0\ M_{solar}$

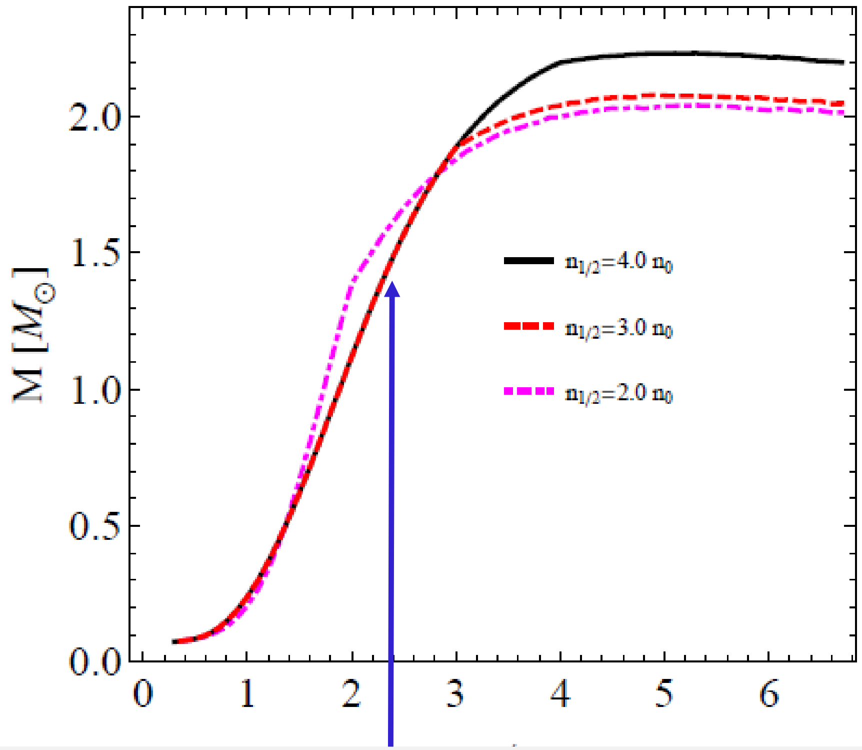

GW data: $\Lambda_{1.4}, R_{1.4} \cdots$ reflect the EoS for $n < 3n_0$, below the topology change, and hence do not directly control the massive stars of $> 2M_{solar}$.

Star properties:GW170817

$$\mathcal{M}=\frac{(M_1M_2)^{3/5}}{(M_1+M_2)^{1/5}}=1.188\,M_\odot.$$

$$\tilde{\Lambda}=\frac{16}{13}\frac{(m_1+12m_2)m_1^4\Lambda_1+(m_2+12m_1)m_2^4\Lambda_2}{(m_1+m_2)^5},$$

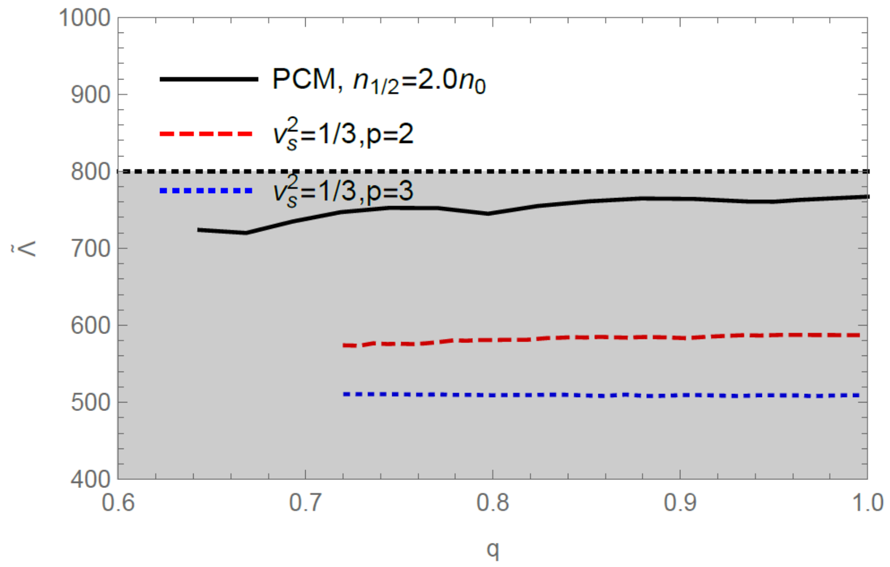

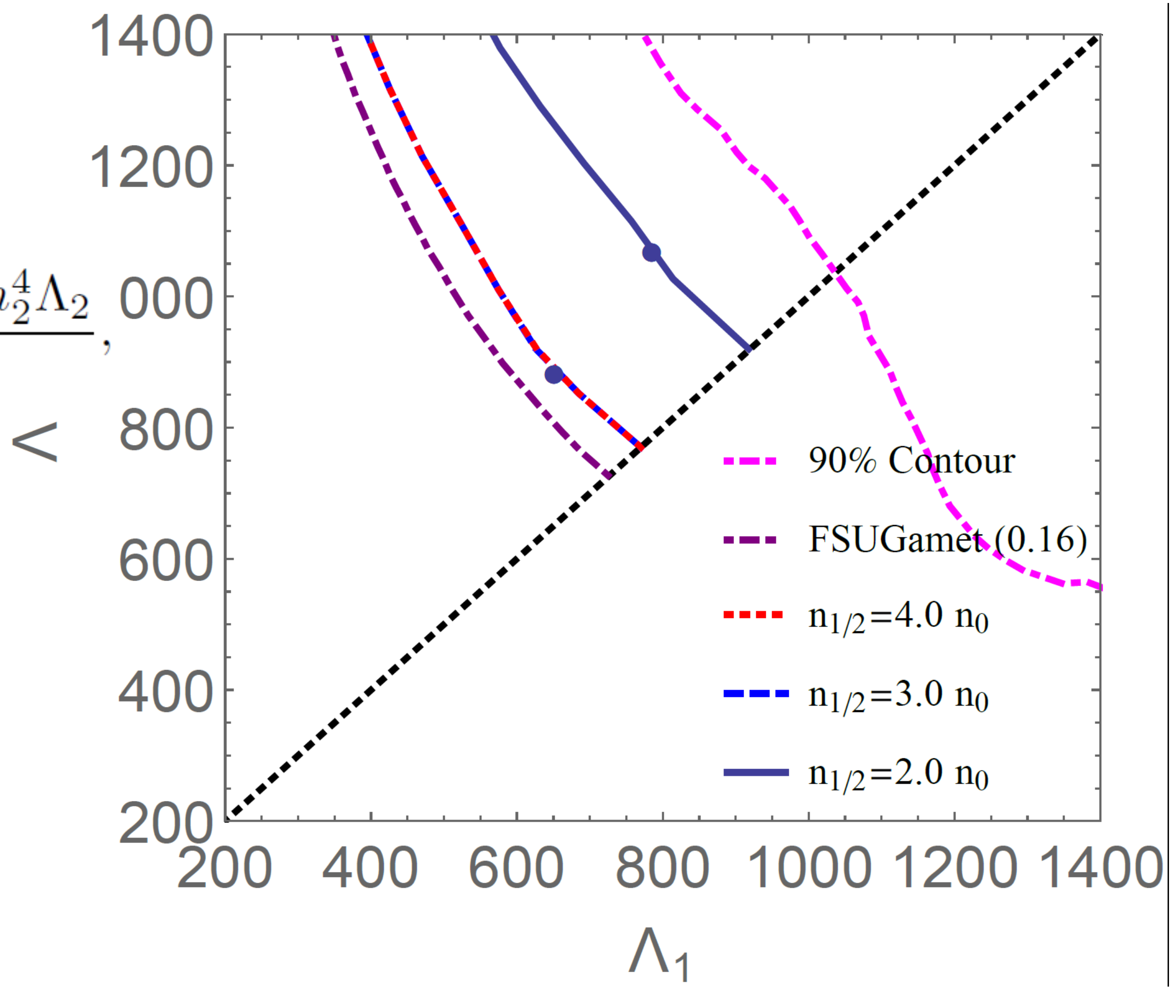

Star properties:GW190425

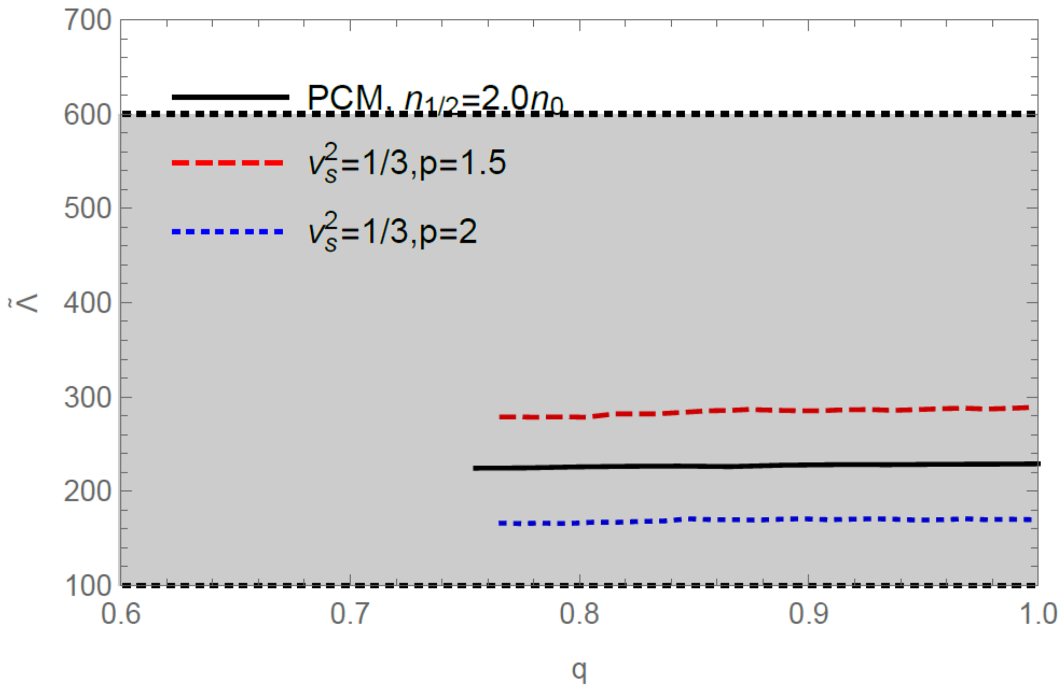

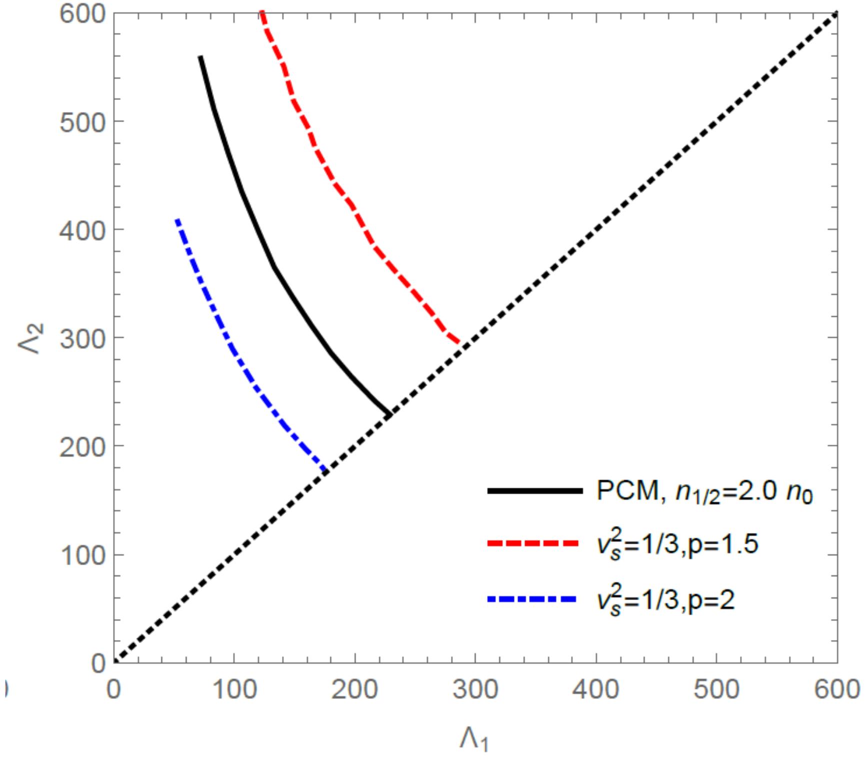

YLM & Rho, 2103.00744, invited review for AAPPS Bulletin

Information from GW190814

Hangzhou Institute For Advanced Study,UCAS

$$P(\mathcal{E}) = \begin{cases} P_{\rm crust}(\mathcal{E}), & \mathcal{E} \le \mathcal{E}_{\rm c-edge} \\ P_{\rm NM}(\mathcal{E}), & \mathcal{E}_{\rm c-edge} \le \mathcal{E} \le \mathcal{E}_{\rm tr} \\ \left(\frac{v_{\rm s}}{c}\right)^2 (\mathcal{E} - \mathcal{E}_{\rm tr}) + P_{\rm NM}(\mathcal{E}_{\rm tr}), & \mathcal{E}_{\rm tr} \le \mathcal{E}, \end{cases}$$

Kanakis-Pegios, et al, 2012.09580

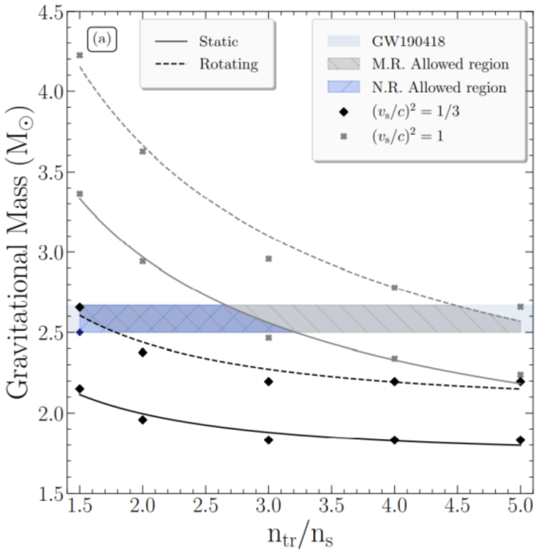

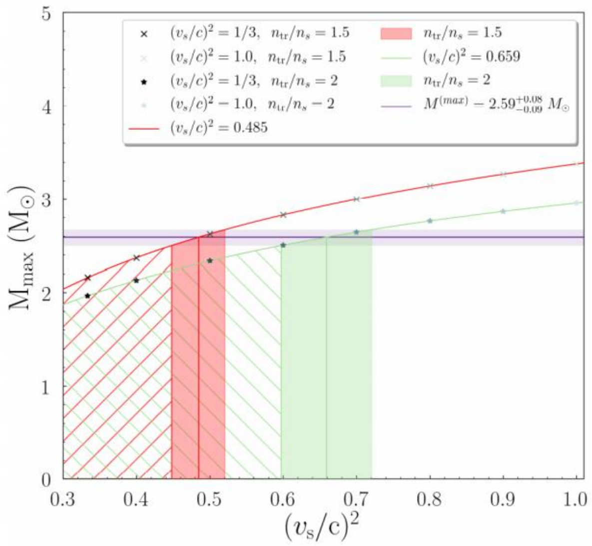

- N.R. 中子星： n_{tr} = [1.5,3.2]n_0; $(v_s\ /c)^2$= [0.45,1]; M. R. 中子星： n_{tr} > 1.6n_0,声速无限制;
- M-vs: $(v_s\ /c)^2$> 1.3;
- TD: tr 越大，TD越小，NS约紧致、越难变形。

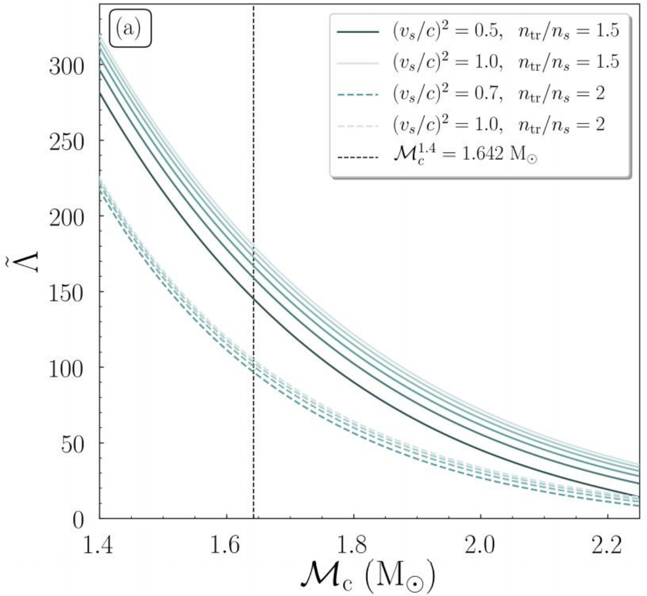

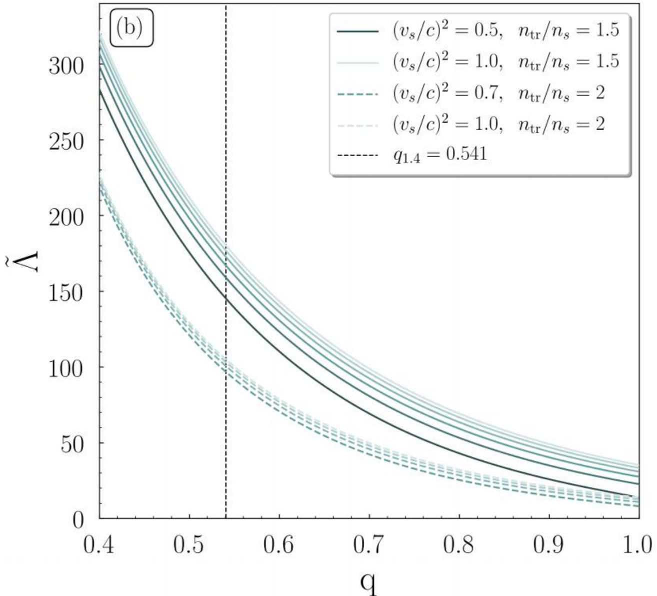

A quark core?

nature physics
LETTERS
https://doi.org/10.1038/s41567-020-0914-9
Check for updates

OPEN

Evidence for quark-matter cores in massive neutron stars

Eemeli Annala[1], Tyler Gorda[2], Aleksi Kurkela[3,4], Joonas Nättilä[5,6,7] and Aleksi Vuorinen[1]

The theory governing the strong nuclear force—quantum chromodynamics—predicts that at sufficiently high energy densities, hadronic nuclear matter undergoes a deconfinement transition to a new phase of quarks and gluons[1]. Although this has been observed in ultrarelativistic heavy-ion collisions[2,3], it is currently an open question whether quark matter exists inside neutron stars[4]. By combining astrophysical observations and theoretical ab initio calculations in a model-independent way, we find that the inferred properties of matter in the cores of neutron stars with mass corresponding to 1.4 solar masses ($M_\odot$) are compatible with nuclear model calculations. However, the matter in the interior of maximally massive stable neutron stars exhibits characteristics of the deconfined phase, which we interpret as evidence for the presence of quark-matter cores. For the heaviest reliably observed neutron stars[5,6] with mass $M \approx 2M_\odot$, the presence of quark matter is found to be linked to the behaviour of the speed of sound c_s in strongly interacting matter. If the conformal bound $c_s^2 \le 1/3$ (ref. [7]) is not strongly violated, massive neutron stars are predicted to have sizable quark-matter cores. This finding has important implications for the phenomenology of neutron stars and affects the dynamics of neutron star mergers with at least one sufficiently massive participant.

limit of very high densities, perturbative-QCD (pQCD) techniques, rooted in high-energy particle phenomenology and built on deconfined quark and gluon degrees of freedom[12,13], become accurate, providing the quark-matter EoS to the same accuracy at densities $n \gtrsim 40n_0 \equiv n_{\mathrm{pQCD}}$.

In the above two limits, QCD matter is known to exhibit markedly different properties. High-density quark matter is approximately scale-invariant, or conformal, whereas in hadronic matter the number of degrees of freedom is much smaller and scale invariance is also violated by the breaking of chiral symmetry. These qualitative differences are reflected in the values taken by different physical quantities. The speed of sound takes the constant value $c_s^2 = 1/3$ in exactly conformal matter and slowly approaches this number from below in high-density quark matter[12]. By contrast, in hadronic matter, the quantity varies considerably: below saturation density, CET calculations indicate $c_s^2 \ll 1/3$, while at higher densities most hadronic models predict $\max(c_s^2) \gtrsim 0.5$. The polytropic index $\gamma \equiv \mathrm{d}(\ln p)/\mathrm{d}(\ln \epsilon)$, on the other hand, has the value $\gamma = 1$ in conformal matter, while both CET calculations and hadronic models generically predict $\gamma \approx 2.5$ around and above saturation density. Finally, the number of degrees of freedom is reflected in the pressure normalized by that of free quark matter (the Fermi-Dirac (FD) limit), p/p_{FD} (ref. [12]). This quantity obtains values of order 0.1 in CET calculations and hadronic models,

the values of γ as a good approximate criterion. Given that $\gamma = 1.75$ is both the average between its pQCD and CET limits and very close to the minimal value the quantity obtains in viable hadronic models (see Fig. 2 and our discussion in the Methods), we are led to choose the following criterion for separating hadronic from quark matter: given an interpolated EoS, the smallest density from which γ is continuously less than 1.75 to asymptotic densities is identified with the onset of quark matter. We emphasize, however, that this is

In conclusion, our model-independent analysis has demonstrated that the existence of quark cores in massive NSs should be considered the standard scenario, not an exotic alternative. For all stars to be made up of hadronic matter, the EoS of dense QCD matter must be truly extreme. This view is also consistent

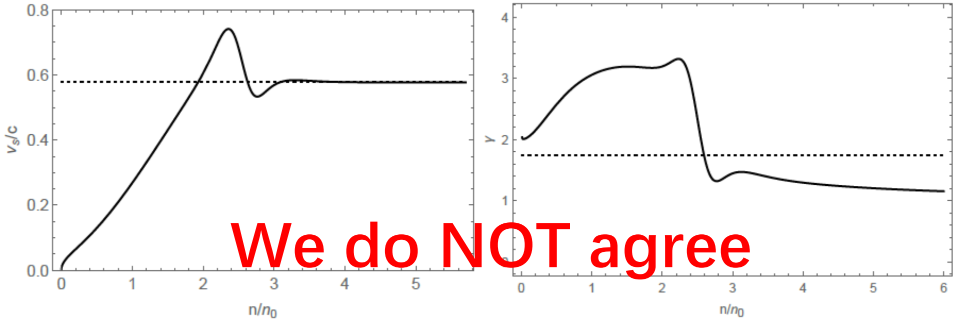

We do NOT agree

FIG. 1. Density dependence of the SV of stars v_s (left panel) and the polytropic index $\gamma = d\ln P/d\ln\epsilon$ (right pannel) in neutron matter.

YLM & M. Rho, 2006.14173

NOT made of quark, but exotic objects with baryon number-1/2! anyon?

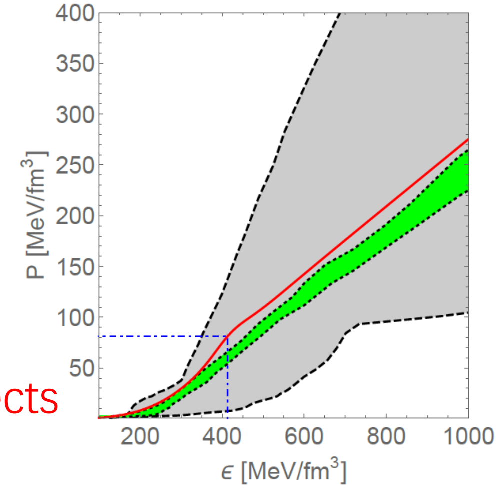

FIG. 2. Comparison of (P/ϵ) between the PCM velocity and the band generated with the SV interpolation method used in [23]. The gray band is from the causality and the green band from the conformality. The red line is the PCM prediction. The dash-dotted line indicates the location of the topology change.

Other models

Quark-hadron crossover

$$P(\mu) = S(\mu)P_q(\mu) + (1 - S(\mu))P_h(\mu)$$

Quarkyonic matter

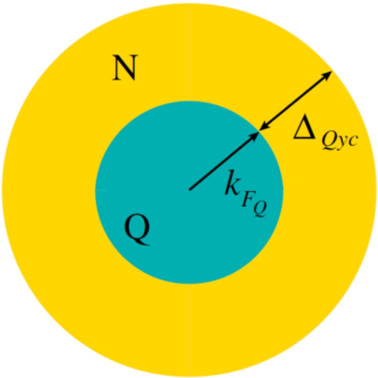

Quarkyonic matter

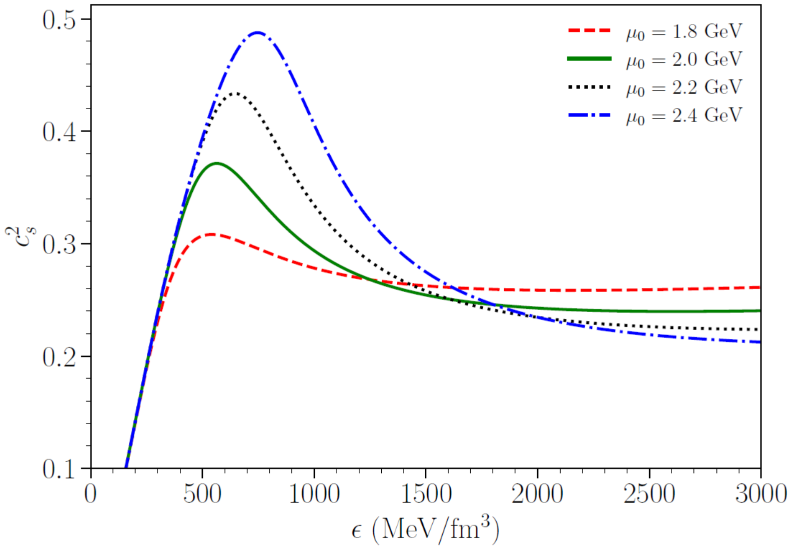

Kapusta & Welle, 2103.16633

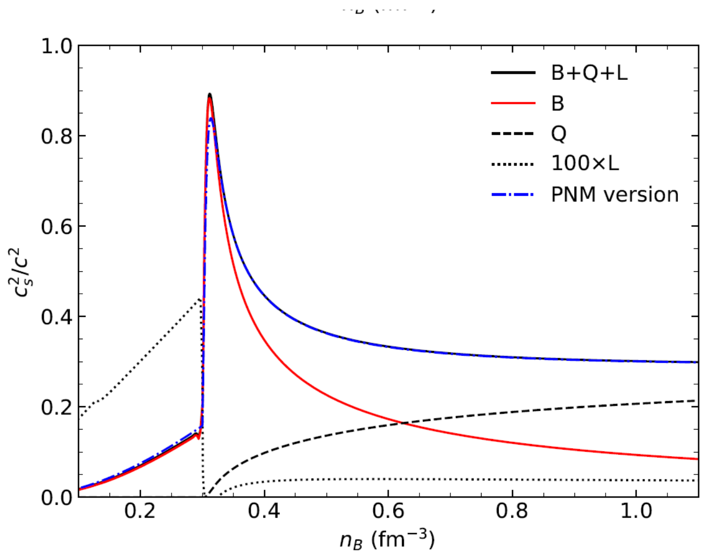

Zhao & Lattimer, 2004.08293

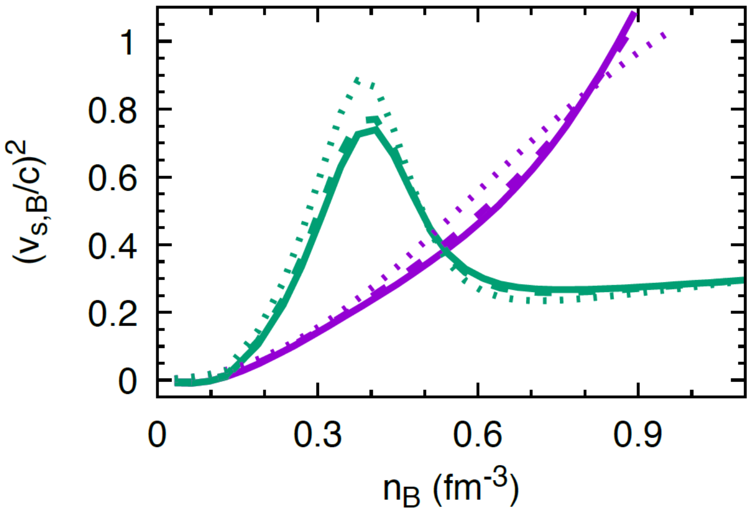

Margueron et al, 2103.10209

Hadronic phase

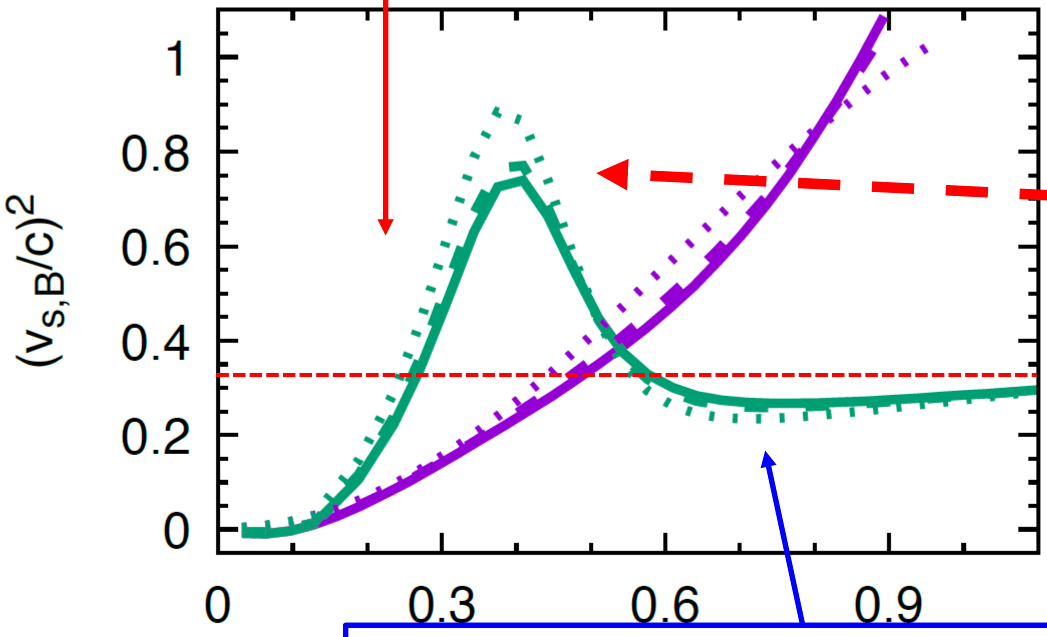

Emerges in the transition from a phase with broken chiral symmetry to one with gapped Fermi surface with the condensation of diquarks and dibaryons.

Gas of non-int. massless particles; zero baryon chemical potential hQCD; LQCD.

Hippert, *et al.* , 2105.04535

Diagnose EoS using GW waveforms

A typical evolution can be divided in three (or four) phases:

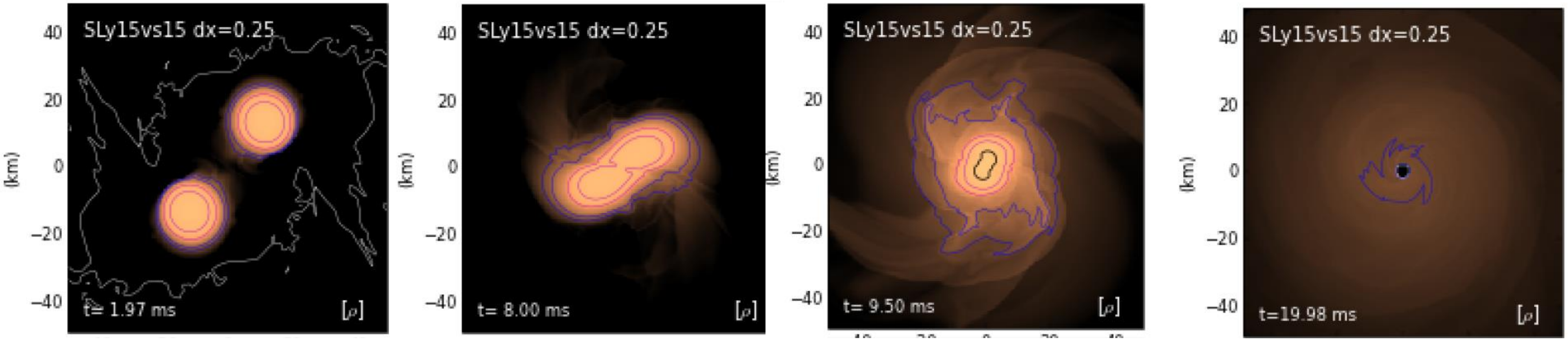

The inspiral phase

The merger phase:
The two stars come into contact, compressing their matter and giving rise to a complex hydrodynamical phen.

The post-merger phase:
The neutron star formed during the merger evolves, with a different phen. depending on its mass, EOS, and angular momentum distribution. The remnant star is bar-deformed, rotates differentially, and emits GWs with high luminosity

The collapse phase:
If the merger remnant has a mass greater than the limit for a non-rotating neutron star imposed by its EOS, the neutron star collapses to a black hole, when its rotation has slowed down enough.

Bauswein and Stergioulas 2015 PRD91 124056.

Diagnose EoS using GW waveforms

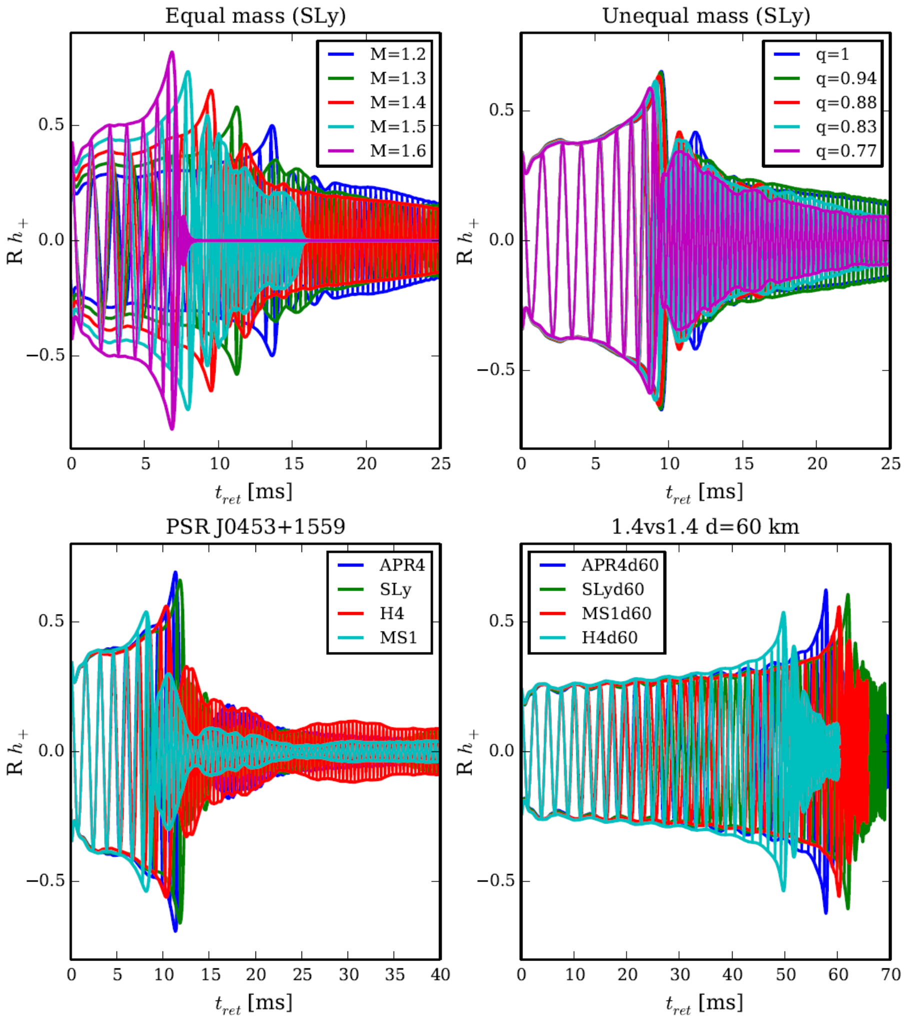

K. Hotokezaka, et. al., PRD 87 044001

- In the first phase (the so called inspiral phase) the GWs progressively increase both their frequency and amplitude, generating a signal known as “chirp". The point of maximum amplitude is conventionally defined as the merger of the two stars.
- After the merger, the signal amplitude drops and then its amplitude raises again, at a higher frequency, which strongly depends on the EOS, for the GW emission due to the rotation of the bar-deformed neutron star remnant.
- The post merger GW emission amplitude decreases exponentially, due to the redistribution of angular momentum and the star approaching a more axisymmetric state, but it shows in some models interesting features, which will be analysed later.
- The models collapsing to black hole are clearly recognizable, because after collapse the GW amplitude drops immediately to negligible values.

Diagnose EoS using GW waveforms

国科大杭州高等研究院
Hangzhou Institute For Advanced Study,UCAS

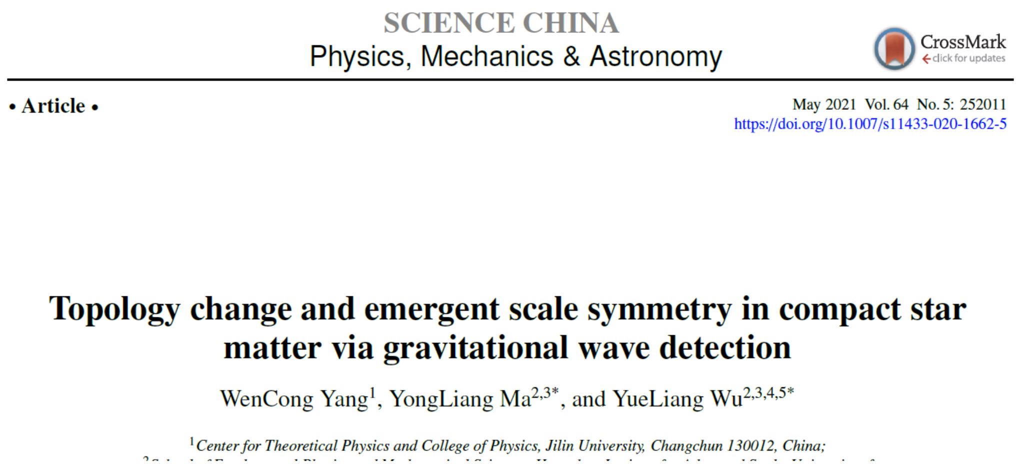
SCIENCE CHINA
Physics, Mechanics & Astronomy
CrossMark

• Article •

May 2021 Vol. 64 No. 5: 252011
https://doi.org/10.1007/s11433-020-1662-5

Topology change and emergent scale symmetry in compact star matter via gravitational wave detection

WenCong Yang[1], YongLiang Ma[2,3*], and YueLiang Wu[2,3,4,5*]

[1]Center for Theoretical Physics and College of Physics, Jilin University, Changchun 130012, China;

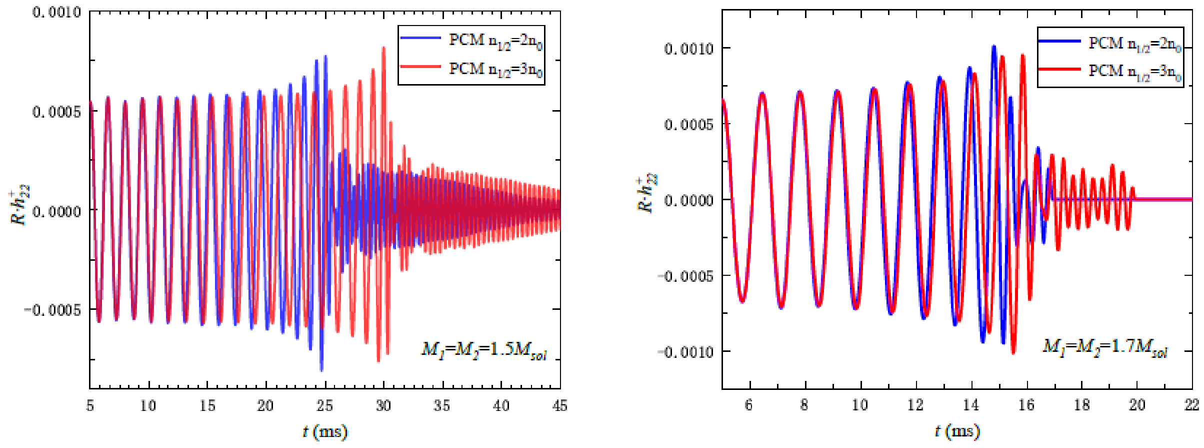

(a)

(b)

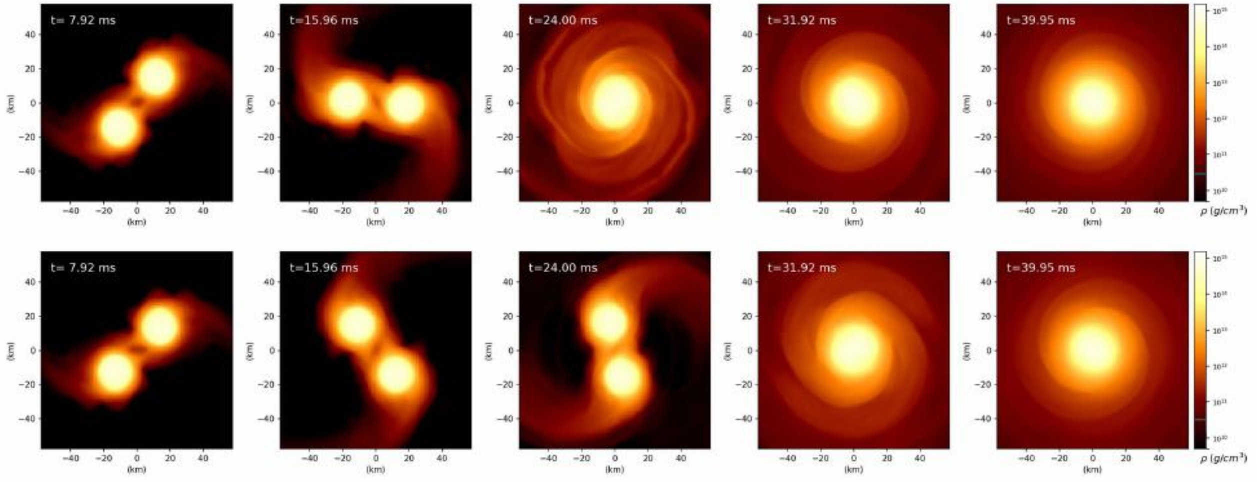

Estimate the location of $n_{1/2}$ using GWs emitted from BNS merger;

- 物态方程越硬，物质交换越难；
- 物态方程越硬，共转次数越多；
- 最终产物，中子星或黑洞，依赖于物态方程。

结　论　？

- 引力波天文学时代为致密核物质研究提供的新的检验平台；
- 中子星质量-半径及潮汐形变的精确测量;

  例如NICER正在进行的关于大质量脉冲星 PSR J0740+6620 半径的测量;

  S. Guillot, et al. 1912.05708.

- 地面高频引力波的精密测量;
- ……

Thank you for your attention!

Comments are welcome!

- The β' is responsible for the scalar mass which is important in nuclear interactions so it cannot be zero.
- The deviation from the LOSS approximation arises from the c_i coefficients with $c_i < 1$.That the LOSS seems to work well in the EoS for nuclear matter in the $\boldsymbol{G\sigma EFT}$ approach could be taken as an indication for $c_i \approx 1$.
- If, however, dense matter is described in the HLS Lagrangian put on crystal, it was realized that unless the c_i coefficient in the homogeneous WZ (hWZ) term is $c_{hWZ} < 1$, there can be no chiral transition at high density.

Patterns of scale symmetry in nuclei--g_A quench

Why the Gamow-Teller (GT) transition in the simple shell model in nuclei requires a quenching factor $q \sim (0.75 - 0.80)$ multiplying the axial coupling constant $g_A^{free} = 1.276$

$$g_A^{eff} = g_A^{free} \times q \to 1.0$$

J. T. Suhonen, Front. in Phys. 2017;
J. Engel, et al., Rept. Prog. Phys. 2017'.

- Could signal certain thus-far unrecognized intrinsic properties of the underlying theory currently accepted, QCD?
- Just a coincidental outcome arising entirely from mundane strong nuclear correlations?
- Combination of both?

- In LOSS approximation, it has been shown that the quenching factor in $g_A^{eff} \approx 1$ is **given predominantly, if not entirely, by standard nuclear correlations**, with little corrections from intrinsic QCD effects.

Y. L. Li, et al., PRC 18' CPC 18'

- Any significant **deviation** from $g_A^{eff} \approx 1$ would then **have to be considered as a signal for scale-symmetry (explicit) breaking**, a quantum anomaly, in terms of the anomalous dimension β' of the gluonic stress tensor $Tr\ G_{\mu\nu}^2$.